Involvement of the L6–7 Loop in SERCA1a Ca 2+ -ATPase Activation by Ca2+ (or Sr2+) and ATP

Guillaume Lenoir, Martin Picard, Jesper Møller, Marc Le Maire, Philippe Champeil, Pierre Falson

Involvement of the L6-7 loop in SERCA1a Ca^{2+}-ATPase activation by Ca^{2+} (or Sr^{2+}) and ATP.

Guillaume Lenoir[1], Martin Picard[1], Jesper V. Møller[2], Marc le Maire[1], Philippe Champeil[1] and Pierre Falson[1,3].

1. Unité de Recherche Associée 2096 of the Centre National de la Recherche Scientifique and Section de Biophysique des Fonctions Membranaires, Département de Biologie Joliot Curie, CEA Saclay, 91191 Gif-sur-Yvette Cedex, and Laboratoire de Recherche Associé 17V and Institut Fédératif de Recherches 46, Université Paris Sud, France.

2. Department of Biophysics, University of Aarhus, DK-8000 Aarhus C, Denmark.

3. To whom correspondence should be addressed: +33 1 69089882 (tel), +33 1 69331351 (Fax), pierre.falson@cea.fr.

Running title: Role of L6-7 loop for SERCA1a Ca^{2+}-ATPase function

Key words: SERCA1a ATPase, P-type ATPase, L6-7 loop, calcium, strontium, fluorescence.

Summary (250 words max)

Wild-type (WT) and Asp813Ala-Asp818Ala (ADA) double mutant of the L6-7 loop of SERCA1a ATPase were expressed in yeast, purified and reconstituted into lipids. In a *solubilized* state, ADA was poorly sensitive to calcium, contrarily to the *reconstituted* state which displayed a maximal calcium-dependent ATPase activity at high ATP concentration (1 mM) close to that of WT. However, monitoring Ca^{2+} binding of each reconstituted ATPase in the absence of ATP by intrinsic or extrinsic fluorescence revealed a true affinity for calcium binding of 8 µM for ADA, 20-30-fold lower than that of estimated for WT (0.3 µM). At low ATP concentration (2 µM) and saturating Ca^{2+} concentrations ADA was nevertheless only poorly phosphorylated and displayed a large reduction of calcium-dependent ATPase activity. Transient kinetics experiments revealed an overshoot in the ADA phosphorylation level, primarily arising from a large reduction of the Ca^{2+}-induced E2 to E1 transition rate. Furthermore, at high ATP concentration (1 mM), ADA had in fact a higher sensitivity to vanadate than WT, consistent with an increased concentration of the "E2" unphosphorylated form during turnover. ADA also proved to have a reduced affinity for ATP equilibrium binding in the absence of Ca^{2+}. This study, the first performed with a purified mutant of ATPase, reveals the central role of the L6-7 loop in coordinating events in the transmembrane and cytosolic domains. Particularly, it reveals the involvement of the L6-7 loop in the process that leads to acceleration of Ca^{2+} binding by ATP binding to dephosphorylated ATPase.

Introduction

Muscle relaxation is due to the removal of calcium from the cytosol and its accumulation into sarcoplasmic reticulum (SR) through an active transport consuming ATP (1,2). In fast twitch muscle this transport is achieved by the SERCA1a isoform of Ca^{2+}-ATPase (3), with a stœchiometry of two calcium ions transported per ATP molecule hydrolyzed (see reviews (4) and (5)). SR Ca^{2+}-ATPase belongs to the family of P-type ATPases, which transport cations such as H^+, Na^+, K^+ or Ca^{2+} across the membrane and share a common mechanism that involves autophosphorylation of the protein (see review (6)). Calcium transport is achieved through a reversible cycle during which the ATPase is thought to sequentially adopt two main conformations (7,8), E1 and E2, with a high and low affinity for calcium, respectively. Ca^{2+}-ATPase in the E2 state is first activated to Ca_2E1 by the binding of two cytosolic Ca^{2+} ions which triggers phosphorylation of the protein from MgATP. The resulting phosphoenzyme, Ca_2E1~P, is "ADP-sensitive", i.e. it is able to re-form ATP in the presence of ADP, but in the absence of ADP the bound calcium ions can no longer be released back to the cytosol and they are therefore described as being "occluded". The Ca_2E1~P phosphoenzyme then undergoes a main conformational change to reach an "ADP-insensitive" E2P state in which the Ca^{2+} binding sites have a lumenal orientation with a markedly reduced affinity for calcium, and from which calcium ions are released into the SR lumen. The E2P phosphoenzyme is finally hydrolysed back to the E2 state and the overall cycle corresponds therefore to completion of the following scheme: E2 → Ca_2E1 → Ca_2E1~P → E2P → E2 (for a review see e.g. (9,10)).

Much effort has gone into determining the structural organization of SR Ca^{2+}-ATPase, from primary structure predictions (11), electron microscopy (12) and three-dimensional (3D) crystallogenesis (13-15) (for a recent review see (16)). Finally, forty years after the discovery of SR Ca^{2+}-ATPase, the structure has been solved at the atomic level, first in a Ca_2E1 state (14) and then in a thapsigargin-stabilized E2 state (15). The enzyme is organized in three cytosolic domains N, P and A, linked by a stalk to the membrane region, which projects with a short domain exposed to the lumen. The membrane domain contains two calcium-binding sites, distant from the phosphorylation (P) and the nucleotide-binding (N) domains, with calcium liganding residues as previously revealed by site-directed mutagenesis (17,18). Comparison of the two 3D-structures shows that the cytosolic domains undergo very large movements, being separated from each other in Ca_2E1 while they are in close contact in E2.

Previously, by combining limited proteolysis and site-directed mutagenesis, we have drawn attention to the cytosolic L6-7 loop (F809-S830), connecting transmembrane segments 6 and 7 (19-21). Cluster mutations D813A-D818A (ADA) or D813A-D815A-D818A (AAA) in this loop were found to reduce the Ca^{2+}-dependent ATPase activity of the protein in its solubilized state (19) as well as the protein's apparent affinity for calcium, suggesting a role of the L6-7 loop in activation by calcium during the early steps of the cycle (20). Both the ADA mutations and the conservative related ones, D813N-D818N, were then found to reduce the amount of calcium bound to the protein at intermediate concentrations of Ca^{2+} (22). At this point, evidence was obtained from the 3D-structure of the Ca^{2+}-ATPase that the L6-7 loop is located too far away from the two high affinity calcium binding sites to participate directly in the binding of calcium to these sites. This was confirmed by the fact that wild type (WT) and mutant (ADA) ATPases were both able to occlude calcium in the presence of Cr.ATP (21). Moreover, a detailed site-directed mutagenesis study of several residues of the L6-7 loop highlighted its role in stabilizing the ATPase structure through an extended network of hydrogen bonds (23). A comparable study carried out with Na^+,K^+-ATPase revealed that removal of the negatively charged residues in this loop only had a moderate effect on the affinity of the enzyme for potassium, and simultaneously revealed the higher sensitivity of these mutants to SDS (24). The reduction of the cation-binding ability of the Ca^{2+}-ATPase L6-7 loop after mutation was nevertheless confirmed by studying a chemically synthesized peptide

corresponding to the L6-7 loop (G808-P827) which was found to interact with calcium and to bind lanthanum, in contrast with a related peptide in which an AAA cluster mutation had been introduced (21). The L6-7 loop was thus suggested to provide an entrance port for calcium, with the negatively charged aspartic residues involved in a pre-binding site (21) and recent computer simulations led to the same conclusion (25). However this proposal remains a matter of debate since Andersen and colleagues have recently reported that single D813L mutation in L6-7 and K758I in the 5th membrane span both result in a similar kinetic behaviour (26). From all these experiments it appears that the L6-7 loop is functionally important, but in a way which still remains unclear and needs to be further clarified.

In the present work, we characterize WT and ADA ATPases by using classical approaches for these expressed proteins and also by monitoring ATPase conformational changes by intrinsic or extrinsic (FITC) fluorescence. The fluorescence approaches require a rather high level of protein purity, which could be obtained by using an improved yeast overexpression system (27) together with a recently developed procedure (28,29) to purify and reconstitute into lipids the expressed WT and mutated ATPases. The present results show that in a solubilized state, the ADA mutant experiences a dramatic decrease of its calcium-dependent ATPase activity. On the contrary, reconstituted in a lipid environment, it displays an almost unaltered maximal calcium-dependent ATPase activity at saturating Ca^{2+} and high ATP, with an apparent affinity for Ca^{2+} altered only moderately. In the absence of ATP, the true affinity of ADA for Ca^{2+} is however more seriously reduced (20-30 fold) compared to WT. The apparent affinity for phosphorylation from Pi in the absence of Ca^{2+} is unaltered in the mutant, but the transition from the Ca^{2+}-free to the Ca^{2+}-bound form of the ATPase is apparently slowed down quite significantly, as manifested by several criteria. In addition, we also obtain evidence for a slightly enhanced overall rate of dephosphorylation and a reduced true affinity for ATP binding to the ADA mutant in the absence of Ca^{2+}. We conclude on the basis of our data that the L6-7 loop is involved in an interplay between the ATP and Ca^{2+} binding sites, primarily to allow ATP to accelerate the E2 to E1Ca_2 transition taking place before phosphorylation.

Experimental procedures

Materials

The electrophoresis miniprotean 3, transblot module, GS-700 densitometer, Molecular Analyst software and Bio-beads were from Bio-Rad laboratories. Yeast culture products were from Difco Laboratories. N-dodecyl-β-D-maltoside (DDM) was from Anatrace Inc (Anagrade) and $C_{12}E_8$ was from Nikko Chemical Co (Tokyo). Low molecular weight markers and PD-10 columns were from Amersham Biosciences. Other products were purchased from Sigma-Aldrich Corp. The STORM 860 Phosphorimager was from Molecular Dynamics. The rapid mixing QFM5 device was from Biologic, Chaix, France. The Multiskan Bichromatic spectrophotometer was from Labsystems. The Sigmaplot software was from SSPS, Inc. The SimZyme software was a kind gift from Dr. Jens Peter Andersen (Aarhus, Denmark).

SR membrane preparation

SR vesicles were isolated from rabbit skeletal muscle according to de Meis & Hasselbach (30) and Champeil *et al*. (31). Before the preparation, the rabbits were subjected to a 48 h-starvation diet (32).

Expression of WT and ADA SERCA1a Ca^{2+}-ATPase species in yeast

The methods used for construction of expression plasmids, cultures and preparation of membrane fractions were described previously (20,28). After induction by galactose of SERCA expression, yeast cells were broken and the light membrane fractions containing the expressed Ca^{2+}-ATPase were collected by differential centrifugation and stored in a medium containing 10 mM Hepes-Tris pH 7.5, 0.3 M sucrose and 0.1 mM $CaCl_2$.

Purification of C-terminal His-tagged Ca^{2+}-ATPase

Expression and purification of WT and ADA ATPases were as described previously (28), with the following modifications during purification: (i) ADA Ca^{2+}-ATPase was solubilized with DDM at a detergent:protein ratio of 5:1 (w/w) instead of 3:1, (ii) after Ni^{2+}-NTA affinity chromatography the buffer of the pooled His-tagged Ca^{2+}-ATPase was exchanged, using a PD-10 device, with buffer of the following composition: 25 mM Mops-Tris pH 7.0, 40 % glycerol, 1 mM $CaCl_2$, 1 mM $MgCl_2$, 0.5 mg/ml DDM, 1 mM DTT, 0.1 M KCl and 0.25 mg/ml of an egg yolk lipid suspension. The lipid suspension was made up of a 10:1 ratio (w/w) of L-α-phosphatidylcholine (EYPC) and phosphatidic acid (EYPA), the resulting vesicles being homogenized to a size of 100-300 nm by passing the suspension through a filter device (Avestin, Hamilton) calibrated to 100 nm (33). The lipid concentration in the PD-10 pool was increased to 1 mg/ml by using the same EYPC-EYPA suspension, and DDM was then removed by adding 200 mg of Bio-beads per mg of detergent and gently stirring for 3 hours. The size of the resulting reconstituted fragments was checked by freeze fracture electron microscopy (by courtesy of Jean-Marc Verbavatz, CEA Saclay). Aliquots of the purified fraction were frozen in liquid nitrogen and stored at –80 °C. Purity was checked by SDS-PAGE after Coomassie blue staining, and quantitation of expressed Ca^{2+}-ATPase was performed with a GS-700 densitometer, using rabbit SR Ca^{2+}-ATPase as standard.

ATPase activity measurements.

Spectrophotometric measurements of ATP hydrolysis by the Ca^{2+}-ATPase was routinely performed at 20 °C with an ATP-regenerating coupled enzyme assay originally described by Pullman and co-workers (34) and subsequently adapted (35,36). The reaction was performed in 2 ml of a medium containing 50 mM Tes-Tris, pH 7.0, 50 mM KNO_3, 7 mM $MgCl_2$, 1 mM

phosphoenolpyruvate, 0.1 mg/ml pyruvate kinase, 0.1 mg/ml lactate dehydrogenase, an initial concentration of about 0.3 mM NADH, 3-6 µg/ml of purified Ca^{2+}-ATPase and 0.1 mM total $CaCl_2$. When needed, EGTA was added to yield the desired $[Ca^{2+}]_{free}$ (37), using a Ca^{2+}-EGTA apparent dissociation constant of about 0.5 µM in the presence of 7 mM $MgCl_2$ (0.4 µM in the absence of Mg^{2+} at pH 7.0). The reaction was initiated by addition of either 2 µM or 1 mM Na_2ATP, as indicated. When indicated, a solubilizing concentration of 1 mg/ml of octaethylene glycol monododecyl ether ($C_{12}E_8$) was added to the ATPase assay medium.

For studies of steady-state inhibition by vanadate, the ATPase activity was estimated from the amount of Pi liberated by a colorimetric assay. In that case, 2 µg/ml of sarcoplasmic reticulum membranes or 4 µg/ml purified and reconstituted WT or ADA ATPase were added to 140 µl of assay medium, containing 50 mM Mops-Tris at pH 7.0 (20 °C), 100 mM KCl, 5 mM Mg^{2+}, 1 mM MgATP, 2 µg/ml A23187, 1 mM phosphoenolpyruvate, 0.1 mg/ml pyruvate kinase and 100 µM total Ca^{2+}. Various concentrations of orthovanadate were also added, up to 1 mM. ATP hydrolysis was triggered by addition of the membranes and quenched by addition of 70 µl of 10 % SDS, supplemented with 0.05 % antifoam A. Inorganic phosphate was revealed with molybdate by adding 490 µl of a solution prepared by mixing one part of 4 % ammonium molybdate in 15 mM Zinc acetate at pH 5 with four parts of 10 % freshly prepared ascorbic acid, titrated to pH 5 with NaOH. The blue color developed over 90 minutes at room temperature (38,39) was read as duplicates in 96-well microtiter plates, at 690 nm on a Multiskan Bichromatic spectrophotometer. The concentration of phosphate released was calculated from standard curves (0-0.2 mM range) prepared in the absence or presence of vanadate. Note that vanadate inhibition experiments were performed with this phospho-molybdate colorimetric assay and not with the usual coupled enzyme assay in order to avoid artifacts due to the stimulation by vanadate of NADH oxidation, a stimulation that occurs at submillimolar concentrations of vanadate independently of the presence of any hydrolytic activity (40-42) (see also Figure D in Supplemental Material).

Measurement of the ATPase "true" affinity for vanadate at equilibrium was achieved with 0.16 and 0.2 mg/ml of purified and reconstituted WT and ADA ATPases, respectively or 0.1 mg/ml SR membranes, preincubated with different vanadate concentrations for 60-80 minutes in the medium used for storage of the purified and reconstituted ATPases (25 mM Mops-Tris at pH 7.0, 40 % glycerol, 1 mM $CaCl_2$, 1 mM $MgCl_2$, 1 mM DTT and 100 mM KCl), supplemented with 4 mM Mg^{2+}, 5 mM EGTA and 2 µg/ml A23187. Residual ATPase activity was then measured within the first 30 seconds following a 20-fold dilution into a standard enzyme-coupled assay buffer (i.e. before vanadate release). This buffer contained 50 mM Mops-Tris at pH 7.0 (20 °C), 100 mM KCl, 5 mM Mg^{2+}, 1 mM MgATP, 1 mM phosphoenolpyruvate, 0.1 mg/ml pyruvate kinase, 0.1 mg/ml lactate dehydrogenase and 0.3 mM NADH, to which 300 µM total Ca^{2+} had been added to attain 100 µM $[Ca^{2+}]_{free}$ after addition of the preincubated membranes.

Fluorescence measurements.

Fluorescence measurements were performed with a Spex fluorolog instrument. Intrinsic fluorescence was measured with excitation and emission wavelengths of 290 nm and 330 nm and bandwidths of 2 and 20 nm, respectively. The intrinsic fluorescence of SR vesicles or purified and reconstituted WT or ADA Ca^{2+}-ATPase added to the cuvette at about 5 µg/ml was measured at 20 °C in 2 ml of 150 mM Mops-Tris pH 7.0, in the absence of Mg^{2+} (which maximizes the fluorescence signal; see Guillain et al. (43). In these experiments, the free Ca^{2+} concentration was varied by adding appropriate concentrations of EGTA and Ca^{2+}. Monitoring of intrinsic fluorescence changes upon addition of inorganic phosphate was followed by suspending the membranes into a buffer containing 150 mM Mops-Tris (pH 7.0), 20 % Me_2SO, 5 mM $MgCl_2$ and 0.5 mM EGTA; those occuring upon addition of ATP were followed in a medium containing 150 mM Mops-Tris, pH 7.0 (20 °C), 5 mM Mg^{2+}, 55 µM total Ca^{2+} and 2 mM EGTA.

ATPase labelling with fluorescein isothiocyanate (FITC) was performed by incubating SR or reconstituted WT or ADA ATPase (at about 10 µg/ml protein) with 2 µM of FITC, for 10 minutes at 20 °C and pH 8.0. Unbound FITC was eliminated using a PD-10 desalting column, pre-equilibrated with 150 mM Mops-Tris, pH 7.0 and 100 µM $CaCl_2$. FITC-treated samples were then diluted 4-fold in 100 mM KCl, 5 mM $MgCl_2$ and 150 mM Mops-Tris, pH 7.0, and FITC fluorescence measurements were carried out with excitation and emission wavelengths set at 490 and 530 nm, respectively (with 5 nm bandwidths).

Phosphorylation from ATP and Pi, and dephosphorylation experiments

Phosphorylation from [γ-^{32}P]ATP was measured at 20 °C unless otherwise indicated, by adding 2 µM of 2 mCi/µmol [γ-^{32}P]ATP to WT or ADA mutated Ca^{2+}-ATPase at about 2 µg/ml (about 1 µg per assay) in buffer A (50 mM Mops-Tris, pH 7.0 (20 °C), 100 mM KCl, 5 mM Mg^{2+}), supplemented with various concentrations of $CaCl_2$ (or of a Ca^{2+}/EGTA buffer). Phosphorylation measurements in the millisecond-range were performed at 20 °C with a rapid mixing and quenching apparatus. When indicated, ATPase phosphorylation was also measured in the same medium on ice, and dephosphorylation was subsequently triggered by adding 100 µM of non-radioactive ATP, followed by acid quenching (see below). Phosphorylation from [^{32}P]Pi was measured at 20 °C by adding 100 µM of 2 mCi/µmol [^{32}P]Pi to about 10 µg/ml of WT or ADA Ca^{2+}-ATPase (about 1 µg per assay) suspended in 100 mM Mops-Tris (pH 7.0), 20 % Me_2SO, 20 mM $MgCl_2$, 100 µM Ca^{2+} and various concentrations of EGTA. In all cases, the reaction was stopped by acid quenching with trichloracetic acid (TCA) and H_3PO_4, added at final concentrations of 1 M and 67 mM, respectively. Samples were then left on ice for 20 minutes and centrifuged at 28,000x*g* for 25 minutes at 4 °C. Supernatants were discarded and pellets washed with 800 µl of 75 mM TCA and 5 mM H_3PO_4. After centrifugation, the pellets were resuspended by vortexing for one minute in 50 µl of buffer containing 150 mM Tris-Cl pH 6.8, 2 % SDS, 10 mM EDTA, 16 % glycerol, 0.8 M β-mercaptoethanol and 0.04 % bromophenol blue. Aliquots of 20 µl were then loaded onto Sarkadi-type gels (44) for electrophoretic separation as detailed below. Alternatively, pellets were resuspended with 10 % lithium dodecyl sulphate, 5 mM NaH_2PO_4, 0.005 % SDS, 0.3 M β-mercaptoethanol, 20 % glycerol and 0.04 % bromophenol blue, and 20-µl aliquots were subjected to SDS-PAGE as described by Weber & Osborn (45).

Electrophoretic separation of proteins

For the analysis of Ni-NTA purification, proteins were separated on 8 % gels by Laemmli-type SDS-PAGE (46) and stained with Coomassie blue after one hour migration at 25 mA/gel.

Separation of phosphorylated proteins by SDS-PAGE was done by using Sarkadi-type gels as described previously (44,47,48), with the following modifications. The stacking gel contained 4 % polyacrylamide (29:1 acrylamide:bisacrylamide), 65 mM Tris-H_3PO_4 pH 5.5, 0.1 % SDS, 2 % ammonium persulfate and 0.1 % N,N,N',N'-tetramethylethylenediamine (TEMED). The separating gel was a continuous 7 % polyacrylamide gel containing 65 mM Tris-H_3PO_4 pH 6.5, 0.1 % SDS, 0.4 % ammonium persulfate and 0.05 % TEMED. Gels were run at 80-100 V and 10 mA/gel for about 3 h at 4 °C. The running buffer contained 0.1 % SDS and 170 mM Mops-Tris at pH 6.0, and was kept under stirring during electrophoresis. After electrophoresis, gels were stained and fixed for 10 minutes in 40 % methanol, 10 % acetic acid and 0.1 % Coomassie blue R250. Excess of dye was removed in 10 % acetic acid, 10 % methanol and 1 % glycerol. The gels were dried overnight between two sheets of cellophane paper. Radioactivity was revealed with a STORM 860 Phosphorimager and quantified by comparison with known amounts of [γ-^{32}P]ATP or [^{32}P]Pi. When indicated, samples were also run on acidic gels according to the method of Weber & Osborn (45).

Protein estimation

Proteins were estimated by using the bicinchoninic acid procedure (49) in the presence of 0.1 % SDS. The expressed Ca^{2+}-ATPase was quantified after SDS-PAGE by immunodetection as described previously (20).

Data analysis

The SigmaPlot program (SPSS, Inc.) was used to fit to a Hill equation the data displayed in figures 2, 4, 6C, 7 and 8. The kinetic simulation software SimZyme (50,51) was used to simulate the amount of phosphoenzyme formed as a function of time.

Results

Purification and reconstitution of wild-type and Asp813Ala-Asp818Ala SERCA Ca^{2+}-ATPases expressed in yeast

Wild-type (WT) and Asp813Ala-Asp818Ala (ADA) mutated Ca^{2+}-ATPases were expressed and purified as described in "Experimental Procedures", by using a protocol that we recently proposed and which involves Ni-NTA affinity chromatography (28). The hexa-histidine *C*-terminus tag added to Ca^{2+}-ATPase affected neither the expression nor the stability of the WT, as shown before (28). Starting from yeast membranes containing 2 % of expressed Ca^{2+}-ATPase (lane "Mb" in Figure 1), WT and ADA ATPases were purified to about 50-60 % homogeneity (lanes "WT" and "ADA" in Figure 1). Our original procedure involved a second affinity chromatography step on a Reactive Red column, which was omitted here as the purity obtained after the first step was found sufficient for functional characterization of the purified enzymes. Reconstitution of the protein into lipids by detergent removal was necessary to optimize ATPase activity and stability; it allowed us to form lipid vesicles of 100 to 300 nm diameter which contained the reconstituted proteins, as shown by freeze fracture electron microscopy (Figure A in supplemental material, courtesy from Jean-Marc Verbavatz, CEA Saclay). Starting from 400 mg of light membrane proteins containing about 8 mg of expressed Ca^{2+}-ATPase, we prepared approximately 0.6 mg of purified and reconstituted WT or ADA ATPase. As far as we are aware, this is the first report of the purification of a mutated form of SERCA1a Ca^{2+}-ATPase.

Ca^{2+}-dependent ATPase activity of reconstituted or $C_{12}E_8$-solubilized WT and ADA-ATPases.

In our previous work, we had found necessary to add $C_{12}E_8$ to the ATPase assay medium for measuring the activity of expressed Ca^{2+}-ATPase, since the detergent reduces the background due to contaminating ATPases or oxidases present in yeast membrane fractions (19,20). In the present work, the expressed SERCA was purified enough to be separated from most of the contaminants and $C_{12}E_8$ was no longer required. We were thus able to evaluate the activity of reconstituted WT and ADA ATPases both in the presence and absence of detergent.

As can be seen from Figure 2A, in the presence of $C_{12}E_8$ and at 20 °C, the WT enzyme (circles) displayed a maximal velocity of about 1.2 μmol ATP hydrolyzed/mg protein/min, with a K_M for Ca^{2+} of about 1 μM. This apparent affinity is in agreement with results obtained with Ca^{2+}-ATPase prepared from rabbit skeletal muscle (35), while the measured V_{max} is 4-5 times lower than that of rabbit SR Ca^{2+}-ATPase. As previously discussed (28), this reduced V_{max} suggests that part of the ATPase has experienced irreversible inactivation -presumably during purification- while the active fraction behaves in a normal way. Compared to WT ATPase, the ADA mutant (squares) was only weakly activated by increasing Ca^{2+} concentrations, as previously reported (20). As β-D-dodecyl maltoside (DDM) was used throughout the purification procedure, we also tested the effect of that detergent on WT and ADA ATPase activities. As shown in the inset of Figure 2A, DDM was less deleterious for ADA activity than $C_{12}E_8$, although activation by Ca^{2+} remained rather sluggish. For both preparations, activities measured at very low free Ca^{2+} concentrations were similar, and probably arose from residual protein contaminants.

When ATPase measurements were now performed in the absence of detergent, as shown in Panel B of Figure 2, WT ATPase again behaved normally, *i.e*. its V_{max} was essentially unchanged and its K_M for Ca^{2+} was slightly shifted towards higher affinity (about 0.3 μM), as previously found for intact SR ATPase (35). Remarkably, the ADA mutant now displayed a full maximal velocity, with a K_M for Ca^{2+} of 1-2 μM, only moderately higher than that of the WT. The limited effect of the mutation on the K_M for Ca^{2+} is in accordance with the results of Zhang *et al*. (22). Similar results were obtained when the ATPase activity of the purified and reconstituted proteins was assayed with

strontium (52,53), as displayed in the inset of Figure 2B. WT and ADA enzymes had K_M values for Sr^{2+} of 15 and 35 μM respectively, showing that the shift in cation affinity for ADA compared with WT was the same for Ca^{2+} and Sr^{2+}. To investigate whether the recovery in reconstituted ADA of a fairly high affinity for Ca^{2+} or Sr^{2+} was dependent on trapping caused by the negatively charged EYPA used for reconstitution, we repeated the same experiment with an enzyme reconstituted in the presence of EYPC only; but it turned out that the presence or absence of EYPA made no difference (Figure B in Supplemental Material). Hence, the poor sensitivity to Ca^{2+} of the hydrolytic activity of the ADA mutant, shown in panel A and previously reported (20) mainly results from the fact that activity in this Panel was assayed under solubilizing conditions. Solubilization with $C_{12}E_8$, and to a lesser extent with DDM, markedly affects the functional properties of the ADA mutant.

The striking effect of detergent led us to further explore the effect of $C_{12}E_8$ and DDM on enzyme activity during the various stages of the solubilization process by measuring the hydrolytic activity of purified and reconstituted ADA and WT ATPase as a function of $C_{12}E_8$ or DDM concentration. As can be seen in Panel A of Figure 3, an initial reduction of ATPase activity was observed for both WT and ADA ATPases in the presence of low, non-solubilizing concentrations of $C_{12}E_8$, as it is also the case for SR ATPase (54). Solubilizing concentrations of $C_{12}E_8$ (e.g. 0.3 - 1 mg/ml) allowed the WT enzyme to recover full activity, again as for SR ATPase (55). For ADA, however, activity recovery at intermediate concentrations of $C_{12}E_8$ was followed by steep inactivation at higher detergent concentrations. Similar experiments were performed with DDM, as shown in Figure 3B, and revealed a less pronounced effect than that observed with $C_{12}E_8$; high concentrations of DDM also reduced Ca^{2+}-ATPase activity of the WT enzyme, as previously found for SR ATPase (55). An unexpected common effect of both $C_{12}E_8$ and DDM on the ATPase activity of the ADA mutant was that the above-mentioned inhibitory effect of sub-solubilizing concentrations of detergent, previously attributed to local delipidation of the protein (55,56), occurred at a significantly lower detergent concentration (0.05 mg/ml) than for WT (0.1 mg/ml), below the critical micellar concentration (cmc) of each detergent (indicated by an arrow in the Figure). This might suggest less firm interaction of lipids with the ADA mutant.

Ca^{2+}- (and Sr^{2+}-) dependence of conformational changes in unphosphorylated WT or ADA ATPase, as monitored by intrinsic fluorescence.

Because of our initial proposal that the L6-7 loop plays an important role not only for ATPase activation by Ca^{2+}, but also for high affinity Ca^{2+} binding (20), we were surprised by the fact that the ATPase activity for ADA illustrated in Figure 2B only revealed a moderate shift in the apparent K_M for Ca^{2+}. We therefore aimed at measuring by an independent assay the true equilibrium affinity for Ca^{2+} of the ADA mutant. Since changes in the intrinsic fluorescence of SR Ca^{2+}-ATPase have been shown to report on the conformational changes occurring upon calcium binding to the enzyme (57), we took advantage of the relative purity of our reconstituted expressed ATPase to use intrinsic fluorescence to monitor Ca^{2+}-dependent changes, as was also recently done with WT purified SERCA1a Ca^{2+}-ATPase expressed with the *Sf9*/baculovirus system (58). Such measurements were performed at pH 7 in the absence of Mg^{2+} to maximize Ca^{2+}-dependent fluorescence changes (43). As shown in Panel A of Figure 4, starting from a situation where the total Ca^{2+} concentration in the fluorimeter cuvette was approximately 55 μM, the intrinsic fluorescence intensity of the WT enzyme dropped when calcium dissociation from ATPase was triggered by the addition of excess EGTA. The relatively small amplitude of this drop, about 2 % versus 5-6 % for native SR (not shown), is consistent with the presence of protein contaminants in the partially purified preparations, as well as some inactive ATPase. When the free Ca^{2+} concentration in the medium was subsequently raised by sequential additions of Ca^{2+}, the intrinsic fluorescence level recovered up to its initial level (provided a high buffer concentration in these experiments was used in order to minimize pH-dependent changes in the fluorescence of

contaminant or inactivated proteins). From the plot displayed in Figure 4C, the affinity of WT Ca^{2+}-ATPase was estimated to be about 0.3 μM, a value close to that of native SR in the same conditions (0.4 μM), and consistent with that reported previously at pH 7 in the absence of Mg^{2+} (59).

As concerns the ADA mutant, its intrinsic fluorescence also dropped upon calcium dissociation, and finally regained a high intrinsic fluorescence upon addition of moderate concentrations of Ca^{2+}; however, raising the fluorescence to its maximal level required larger free Ca^{2+} concentrations for ADA than for WT (Figure 4A). A similar shift in the affinity of ADA compared with WT was also found when Sr^{2+} instead of Ca^{2+} was added to the Ca^{2+}-free ATPases (Figure 4B). By plotting changes in fluorescence intensity as a function of the free Ca^{2+} concentration (Figure 4C), the equilibrium dissociation constant (*K*d) for Ca^{2+} of the ADA mutant was estimated to about 8 μM, i.e. 20 to 30 times higher than that of the WT enzyme. Despite the absence of Mg^{2+} in the fluorescence assay (Figure 4C) and its presence in the hydrolytic activity assay (Figure 2B), the *K*d for Ca^{2+} binding to ADA (8 μM) deduced from the former assay is significantly higher than the K_M of 1-2 μM deduced from the latter, reflecting the difference between equilibrium and turnover conditions (see below).

Ca^{2+}-dependent or vanadate-dependent conformational changes in FITC-labelled ATPases.

FITC covalently binds to lysine 515, a residue localized in the nucleotide binding domain of SERCA, and makes it possible to follow the conformational changes of the protein occurring in the cytosolic domain. Panel A of Figure 5 shows that FITC bound to WT ATPase responded to Ca^{2+} concentration changes in the expected manner, and that FITC bound to ADA ATPase again revealed a poorer affinity of ADA for Ca^{2+}, compared with WT. Note that changes in fluorescence of bound FITC, here examined in the presence of Mg^{2+} as in (60), suggest *K*d values of about 1 and 10 μM for WT and ADA, respectively (not shown), values which are reasonably consistent with those obtained from the tryptophan fluorescence measurements (Figure 4) done in the absence of Mg^{2+}.

In addition, Panel B in Figure 5 shows that FITC bound to WT ATPase also responded to addition of orthovanadate in the expected way (60). Thus, in the absence of Ca^{2+}, vanadate enhanced the fluorescence of bound FITC, while subsequent addition of a moderate calcium concentration (final free concentration of 100 μM) reduced the fluorescence of FITC back to initial level. FITC-modified ADA ATPase displayed the same behaviour as WT upon addition of EGTA and vanadate, indicating that both proteins undergo the same vanadate-dependent conformational changes in the cytosolic region. Contrarily to WT, however, subsequent addition of 100 μM free calcium was not sufficient to reverse the vanadate-induced conformational state, whereas addition of 1 mM was. Since WT and ADA ATPases bind vanadate with the same affinity at equilibrium as shown below, this is again consistent with a poorer affinity for Ca^{2+} of ADA ATPase, compared to WT.

The ADA mutation therefore shifts the true *K*d for Ca^{2+} binding deduced from the fluorescence measurements by a factor of 20 to 30, larger than the factor of about 3 by which the K_M deduced from steady-state ATPase activities is shifted. This is an indication of significant differences between the enzyme kinetics of the ADA mutant and WT enzymes, the basis of which was explored by examining various partial reactions.

Pi -dependent tryptophan fluorescence changes in WT and ADA ATPases, phosphorylation from ^{32}Pi, and competition with Ca^{2+}.

Conformational changes resulting from phosphorylation from inorganic phosphate in the absence of Ca^{2+} were also monitored by intrinsic fluorescence, as shown in Figure 6A. Sequential addition of Pi to the purified and reconstituted WT enzyme in its Ca^{2+}-free state in the presence of 20 % Me_2SO (at pH 7) increased the tryptophan fluorescence with an amplitude about half of that

obtained in the presence of saturating Ca^{2+}, while subsequent addition of a high calcium concentration restored the initial level. This is in agreement with what was originally reported for the native enzyme (61). ADA underwent similar fluorescence changes upon binding of inorganic phosphate, indicating that the apparent affinity with which Pi raises tryptophan fluorescence was not modified by the ADA mutation ($Pi_{½}$ being roughly estimated to 30-40 μM). Addition of a high Ca^{2+} concentration again further raised the ADA fluorescence, up to the initial level, as expected. Addition of more moderate concentrations of Ca^{2+} were less efficient for ADA than for WT (data not shown), in agreement with the above-mentioned poorer affinity of ADA for Ca^{2+}.

We also directly measured with [^{32}P]Pi phosphorylation from inorganic phosphate of WT and ADA ATPases and the effect of competition with Ca^{2+} on this phosphorylation. Results are displayed in Figure 6B and 6C. For WT, the concentration of calcium for half-inhibition of phosphorylation from Pi was about 2 μM, consistent with previous data (20,62) and as expected slightly higher than the true *K*d for Ca^{2+}, because calcium binding competes with phosphorylation from Pi. For ADA, half inhibition required the addition of 35-40 μM Ca^{2+}, *i.e*. a calcium concentration about 20 times higher than for WT, again consistent with all the above evidence for a lower affinity of ADA ATPase for Ca^{2+}.

These measurements of Pi-derived phosphorylation data in the absence of Ca^{2+} therefore do not reveal any clear implication of the L6-7 loop in the events occurring at the phosphorylation site in the cytosolic domain of the ATPase. A different conclusion was however reached when ATP-dependent phosphorylation was monitored, as described below.

Limited activation of ADA ATPase at low ATP concentration.

We next measured the ability of the purified and reconstituted ATPases to become phosphorylated from ATP at various calcium concentrations, using an ATP concentration (2 μM) low enough to minimize any background noise. Panels A and B in Figure 7 show that under these conditions, the apparent $[Ca]_{1/2}$ for calcium activation of phosphorylation of WT was again submicromolar, as expected (here, approximately 0.7 μM) . There was also a slight further increase in phosphorylation at millimolar concentrations of Ca^{2+}, probably due to CaATP replacing MgATP as ATPase substrate, as described previously (20,63,64). For ADA, the amount of phosphoenzyme formed from ATP at submillimolar Ca^{2+} concentrations remained low, about 20-25 % of that of WT, with an apparent $[Ca]_{1/2}$ for calcium activation of phosphorylation that was roughly estimated to be 30 μM. As in our previous experiments (Figures 3A and 4A in (20)), the phosphorylation level further increased at higher (millimolar) Ca^{2+} concentrations, approaching the same level as for WT ATPase. In our previous experiments, we had estimated that the small amount of phosphoenzyme formed at submillimolar Ca^{2+} concentrations was not significant (Figures 3A and 4A in (20)); however, because of the above demonstration of the ability of ADA to bind low concentrations of Ca^{2+}, we now believe that this small amount is indicative of the turnover properties of the ADA mutant, while the higher phosphorylation level found at very high Ca^{2+} concentrations is due to the stabilization of phosphoenzyme arising from replacement of magnesium by calcium at the hydrolytic site. This conclusion was confirmed by time-resolved experiments, showing that dephosphorylation was slower following an initial phosphorylation at a high Ca^{2+} concentration than following an initial phosphorylation at an intermediate submillimolar Ca^{2+} concentration (Figure C in Supplemental Material).

In trying to understand the apparent discrepancy between the quasi-normal ATPase activity of the reconstituted ADA mutant shown in Figure 2B and the fact that the amount of phosphoenzyme formed from ATP was so strongly reduced for this mutant at submillimolar Ca^{2+} concentrations, we realized that very different concentrations of ATP were employed in the two situations, 2 μM for the phosphorylation assay and 1 mM for the ATPase activity assay. We therefore checked the effect of a low ATP concentration on the hydrolytic activity of ADA ATPase. As displayed in Figure 7C, at 2 μM ATP the V_{max} of ATP hydrolysis of the WT enzyme was 0.7

μmol ATP hydrolysed/mg Ca^{2+}-ATPase/min, corresponding to about 70 % of the V_{max} measured at 1 mM ATP. The K_M for calcium activation was about 0.4 μM, close to the value estimated at the higher ATP concentration (Figure 2B). In contrast, the ADA mutant displayed a much lower V_{max} for Ca^{2+}-dependent activity at 2 μM ATP, about 0.2 μmol ATP hydrolysed/mg Ca^{2+}-ATPase/min, corresponding to only 20 % to that of the WT. The ATPase activity of ADA was thus dramatically reduced compared to that measured at high ATP concentrations, and consequently activation by Ca^{2+} was limited, a behaviour similar to what was observed above in Figure 2A at high ATP, but in the presence of $C_{12}E_8$.

ADA ATPase is stabilized in E2 at low ATP concentration, due to a reduced E2 to Ca_2E1 transition and an acceleration of dephosphorylation.

The above-described combination of a low hydrolytic activity and a low steady state phosphorylation of the ADA ATPase would be consistent with the view that the dephosphorylated form E2 of the enzyme accumulates at steady-state at low ATP concentration. A possible reason for such an accumulation would be a slowing down of the Ca^{2+}-induced transition from the unphosphorylated E2 to the Ca_2E1 form, as previously reported for the D813N-D815N-D818N cluster mutant (23). Subsequently, a similar proposal has been made for the D813L mutant (26). In all these cases, the E2 to E1 transition indeed becomes rate-limiting at low ATP concentration, while this is not necessarily the case at high ATP concentrations since the E2 to Ca_2E1 transition has been shown to be accelerated by bound ATP (65-70). We have evaluated the validity of this hypothesis by checking whether the phosphorylation level of the ADA mutant at a low ATP concentration and a moderate Ca^{2+} concentration can transiently reach a higher value during pre-steady state than during steady state when starting from Ca^{2+}-saturated ATPase. Figure 8A shows that when the time course of phosphorylation from ATP was followed in a sub-second time scale at 20 °C, the WT enzyme reached a maximal phosphorylation level within about 0.1 s and then remained essentially constant during the time course of the experiment. In contrast, the ADA enzyme displayed an *overshoot* in phosphorylation, attaining within 0.1 s a maximal level corresponding to about 40 % of that of the WT enzyme and then declining to a level of 20-25 % of WT after 0.6 s.

A similar behaviour has also been reported for mutants K758I in M5 (71,72) or D813L in L6-7 (26), and interpreted as being due to a reduced rate for the E2 → Ca_2E1 transition. The overshoot reported by these authors was more pronounced than that reported here, which at least partially can be attributed to the higher ATP concentration they used (5 μM, compared to the 2 μM ATP used here) and leading to a faster initial phosphorylation rate. In addition, the more limited extent of our overshoot could also be ascribable in part to an increased rate of dephosphorylation in the double ADA mutant compared to the single D813L mutant, due to the additional D818A mutation in ADA. When we monitored the rate of dephosphorylation of ATPase by a chase with unlabeled ATP (Figure 8B), dephosphorylation of the ADA mutant was indeed moderately enhanced compared with WT, being about three times faster. Such acceleration of dephosphorylation will of course reduce the transient overshoot in phosphorylation, and favour accumulation of E2 during steady-state catalysis. Computer simulation of the transient kinetics of phosphorylation of Panel A was carried out with the SimZyme software (71), reducing the cycle to three main species: E2 → Ca_2E1 → Ca_2EP → E2. An additional constraint placed on these simulations was that steady-state ATP hydrolysis by ADA was requested to remain significantly below that of WT ATPase as a consequence of the low ATP concentration used (Figure 7C). The best values obtained for the rate constants of the three transitions for WT were 20, 14 and 4 s^{-1} respectively. These values are reasonably consistent with those (25, 35 and 5 s^{-1}) calculated from the same kind of experiments with COS cells expressing Ca^{2+}-ATPase and at 5 μM ATP (71). Values obtained for ADA were 1.4, 6 and 10 s^{-1}, suggesting indeed that the E2 → Ca_2E1 reaction step in ADA is slowed down more than 10-fold compared to WT, while the rate of

dephosphorylation $Ca_2E1P \rightarrow E2$ increases 2-3-fold and the rate of phosphorylation $Ca_2E1 \rightarrow Ca_2EP$ drops by about two-fold. The latter changes in rates contribute to making the amplitude of the observed overshoot only moderate.

ADA ATPase sensitivity to orthovanadate during turnover at high ATP concentration also reveals increased accumulation of E2.

We then asked whether accumulation of the E2 form of ATPase during steady state turnover, shown above to occur in the presence of 2 μM ATP as a result of the reduced rate of the E2 to Ca_2E1 transition, also occurs in the presence of a high ATP concentration. To address this question we used the classical procedure of evaluating to what extent ADA turnover is inhibited by orthovanadate, an inhibitor thought to react with the E2 form of ATPase only (e.g. (73)). We therefore measured the ATPase hydrolytic activity in the presence of increasing concentrations of vanadate. Figure 9A shows that the EC_{50} for turnover inhibition by orthovanadate in the presence of 1 mM MgATP was about 20-fold lower for ADA than for WT ATPase (about 4 μM versus about 70 μM), consistent with a higher proportion of the E2 form during steady-state cycling of the ADA mutant, compared to WT.

A prerequisite, however, for this conclusion, is that the true affinity of E2 for orthovanadate is the same in WT and ADA ATPases. To address this question we took advantage of the fact that upon dilution of previously inhibited Ca^{2+}-ATPase, bound vanadate is released fairly slowly, namely over a few minutes (60,74,75). This was checked in preliminary experiments (see Figure E in Supplemental Material). We therefore pre-incubated Ca^{2+}-free ATPase in the presence of various concentrations of orthovanadate for more than one hour, to allow for equilibration at all vanadate concentrations, and deduced the proportion of uninhibited ATPase from the rate of ATP hydrolysis observed during the first 30 seconds after 20-fold dilution of the ATPase into a standard coupled-enzyme assay medium. Figure 9B shows that WT and ADA ATPases were inhibited by vanadate with about the same EC_{50} (about 2 μM), confirming that the higher sensitivity of ADA turnover to vanadate illustrated in Figure 9A probably arises from a larger proportion of E2 present during turnover and not from a different intrinsic affinity for vanadate.

Note that in Panel A and Panel B of Figure 9, vanadate inhibition was found to be slightly more effective for SR than for WT ATPase, with respect to both the extent of inhibition and the EC_{50}. The first fact at least is easily understandable, as essentially all ATPase activity in SR vesicles is due to the SERCA, whereas this is not the case in our partially purified expressed ATPase.

The ADA mutation reduces affinity for ATP at equilibrium.

The fact that ADA at a high ATP concentration has an almost unaltered V_{max} (Figure 2B) implies that the high ATP concentration at least partially compensates for the slowing down of the E2 to $E1Ca_2$ transition, so that the rate of this transition is no longer rate-limiting. Nevertheless the transition is likely to remain slower in ADA than in WT, also at high ATP concentrations, as ADA is more sensitive than WT to inhibition by vanadate. Simulation of the cycle with reasonable values for the rate constants confirmed this qualitative conclusion (data not shown). Still the question remains whether ATP, by binding to the E2 conformation, stimulates the rate of the (intrinsically slower) transition in ADA with the same nucleotide binding affinity as it does in WT.

Monitoring tryptophan fluorescence of purified and reconstituted WT and ADA ATPases, as was done previously for SR vesicles (76), provides a method by which we were able to directly estimate the equilibrium affinity of ATPase for ATP in the absence of Ca^{2+}. This is shown in Figure 10, in which Panel A displays control measurements done with SR vesicles and Panel B the results with WT and ADA ATPases. Although the amplitude of the ATP-induced changes is not much larger than the noise level in the measurements, it is clearly seen that experiencing a perceptible conformational change for ADA mutant requires higher concentrations of ATP than for WT

ATPase. The *K*d of ATP binding to WT ATPase was roughly estimated to be about 2-4 μM under these conditions, similar to that for SR itself, while for the ADA mutant it was obviously larger, probably above 20 μM.

At this step, it may be relevant to point out that the rate of ADA phosphorylation from ATP that we deduced from the analysis of our pre-steady state experiment was moderately slower than that for WT (inset to Figure 8A). Experimentally, a similar slowing down was also found by Zhang *et al*. (77). Although our above-estimated *K*d values for ATP refer to ATP binding in the absence of Ca^{2+}, a similar reduction in affinity might also apply to the binding of ATP to ADA in the *presence* of Ca^{2+}, and this could be responsible in part for the observed reduction in the phosphorylation rate.

Discussion

Detergent sensitivity of ADA ATPase

The importance of the L6-7 loop in the function of SERCA1a Ca^{2+}-ATPase was initially revealed by the fact that replacing aspartic acid residues 813 and 818 by alanine reduced Ca^{2+}-dependent ATPase activity very significantly: under the assay conditions used, the ADA mutated enzyme displayed a very low ATPase activity, amounting to only about 10 % of that for WT ATPase (Figure 5 in (19) and Figure 2 in (20)). At that time, as we were working with yeast microsomal membranes, we found it necessary to add a solubilizing concentration of $C_{12}E_8$ to the medium during the activity measurements to suppress the non-specific hydrolytic activity arising from other proteins present in yeast membranes which made it difficult to unambiguously attribute the small Ca^{2+}-dependent activity (amounting to about 2 % of total activity in the absence of detergent) to expressed SERCA1a. The same ADA mutant enzyme, expressed in COS cells, was later reported by Zhang *et al*. (22) to display a significant Ca^{2+}-dependent ATPase activity, up to about 30 % of that of the WT enzyme, a level of activity that was detected without any detergent added to the medium (Figure 4D in (22)). In the same work, the mutation was also reported to reduce the apparent affinity for calcium, but only to a moderate extent, suggesting for ADA a much better sensitivity to calcium than the millimolar sensitivity that we had described previously on the basis of phosphorylation experiments.

These experimental discrepancies were rather puzzling, but a satisfactory explanation for them now arises from the present work. We have found that after purification and reconstitution into lipids, the ADA enzyme behaves more like WT ATPase when activity is measured in the absence of detergent and at a high ATP concentration, from the point of view of both its apparent affinity for Ca^{2+} and its maximal velocity. In contrast, when activity is tested in the presence of solubilizing concentrations of detergent, the purified mutant displays the same low ATPase activity and poor affinity for Ca^{2+} as we have described previously.

Inhibition by detergent of the ADA ATPase activity seems to be of a reversible nature since the final reconstituted preparation retains activity despite the 18 hour-incubation period, in the purification procedure, during which the ATPase is maintained in a solubilized state in the presence of detergent and Ca^{2+} before reconstitution into lipids. In this respect the ADA mutant resembles WT ATPase for which it is well established that irreversible loss of activity can be avoided during solubilization if the latter is performed in the presence of Ca^{2+} and lipids (36). Compared to WT ATPase, however, a difference is that the activity of ADA enzyme is sensitive to sub-solubilizing concentrations of $C_{12}E_8$ or DDM lower than for WT. Such concentrations induce a reversible decrease of ATPase activity, as initially described for the native Ca^{2+}-ATPase by Andersen *et al*. (54) and de Foresta *et al*. (55,56,78). If, as suggested by de Foresta *et al*., this perturbation is due to partial replacement of tightly associated lipids by detergent (55) and/or possible loss of one of the high affinity calcium-binding sites (56), the increased sensitivity of the ADA ATPase to mild detergent may suggest that specific interactions between the protein and some lipid molecules are weakened or lost in the ADA mutant. It could also be an indication that these lipids are close to the L6-7 loop, with possible consequences for the high affinity calcium-binding sites. Interestingly the replacement of acidic residues of the L6-7 loop of the Na^+,K^+-ATPase by alanine residues was recently reported to make the mutant more labile during extraction by SDS (24). Perhaps the loss of negative charges in all these L6-7 loops mutants (which retain positive charges at the other end of the L6-7 loop) might affect local dipoles which become critical for stability when the lipid water interface is destroyed by solubilization.

The ADA mutation reduces the true *K*d for Ca^{2+} or Sr^{2+} binding and slows down E2 to Ca_2E1 transition, impairments which are partially reversed by high ATP concentrations.

By monitoring the intrinsic fluorescence or the extrinsic fluorescence of purified and reconstituted ATPase at equilibrium in the presence of various Ca^{2+} concentrations (Figures 4 and 5), we found that calcium binding to the ADA enzyme occurs with a *K*d 20-30-fold higher than that for the WT enzyme, being shifted from a submicromolar value up to about 10 μM under standard conditions (at pH 7 in the presence of Mg^{2+}). This reduction in the true affinity for Ca^{2+} of ADA ATPase is confirmed by the data of Zhang *et al*. (22) who found that at a free concentration of 3 μM Ca^{2+} less $^{45}Ca^{2+}$ binds to this mutant than to WT ATPase. This 20-30-fold difference in true Ca^{2+} affinity for ADA versus WT ATPase is seemingly at variance with the smaller 3-fold difference in the apparent affinity (K_M) with which Ca^{2+} activates the ATPase at high ATP concentrations (Figure 2B). However, here it should be realized that the K_M for Ca^{2+} activation may be affected not only by the affinity with which the cation binds at equilibrium but also by the rate constants for the other steps in the cycle (see e.g. (51,79) for examples and simulations). Thus the findings that the ADA mutant has retained full ability to bind Ca^{2+} with a reduced affinity, whereas steady-state measurements performed at low ATP hardly reveal any activation by Ca^{2+} of either steady-state phosphorylation or ATPase activity (under these conditions, EP_{max} and V_{max} are much smaller for ADA than for WT, see Figure 7), can be easily understood on the basis of the reduced rate of the transition between the Ca^{2+}-free E2 and Ca^{2+}-bound E1 forms of ADA ATPase (Figure 8A). This transition, which accompanies calcium binding, is an intrinsically fairly slow reaction, which is accelerated very significantly by low levels of ATP, so that at high ATP under usual assay conditions this step is no longer rate-limiting for the entire cycle (65,67,68,70,80,81). With WT ATPase this situation already occurs at 2 μM ATP, resulting in phosphorylation of the enzyme at a high level. This is clearly not the case for the ADA mutant, whose E2 to Ca_2E1 transition rate has been significantly reduced (Figure 8A and (77)). However a high ATP concentration such as 1 mM succeeds in relieving this rate limitation (simulation not shown). In other words, a high ATP concentration overcomes the functional deficiencies due to the mutation. For the ADA mutant in the absence of ATP, this reduced rate of the E2 to Ca_2E1 transition of course contributes to a shift towards a lower affinity of this mutant for Ca^{2+} at equilibrium.

Further consequences of the ADA mutation on the rest of the cycle, and role of the L6-7 loop at the molecular level.

We showed previously that the L6-7 loop plays a major role in ATPase activation by Ca^{2+} (20), and some of these early results advocated a direct role of D813 and D818 in the initial binding of Ca^{2+}, perhaps as an entrance gate, a hypothesis explored further in direct metal binding experiments (21). Along this view, which was also adopted in an *in silico* study (25), the present findings that the ADA mutation reduces the overall ATPase affinity for Ca^{2+} and for Sr^{2+} to the same extent (Fig C in Supplemental Material versus Figure 4A, and inset versus main panel in Figure 2B) suggests that the putative L6-7 pre-binding site (21) does not have any preference for Ca^{2+} over Sr^{2+}. Conversely, since the *rate* of the E2 to Ca_2E1 transition is generally thought to be rate-limited not by Ca^{2+} binding *per se* (or even dehydration) but, instead, by a conformational transition, proposed to occur either *after* binding of the first Ca^{2+} ion (80) or *before* binding of the first Ca^{2+} ion, which in that case corresponds to proton deocclusion from "E2", e.g. (82,83). The fact that the ADA mutation reduces the *rate* of this transition seems to favour the alternative hypothesis, i.e. an *indirect* effect of the mutation (this would account equally well for the similar reduction in affinity for Ca^{2+} and Sr^{2+}). At this stage, it is nevertheless probably fair to leave both hypotheses open.

As regards the effect of the mutation on other steps in the cycle, we found that the ADA mutation leaves the affinity for phosphorylation from Pi almost unaltered (see Figure 6), but increases the dephosphorylation rate after phosphorylation from ATP (presumably by accelerating

the Ca_2E1P to E2P transition) (Figure 8B). In addition, the mutation causes a reduction in the affinity with which MgATP is bound to the ATPase in the absence of Ca^{2+} (Figure 10) -the reduced affinity for ATP binding of the ADA mutant of course contributing to the reduction in the phosphorylation level and the ATPase activity observed, at low ATP (Figure 8)-. These facts illustrate that the L6-7 loop controls other steps in the ATPase cycle, beyond the E2 to Ca_2E1 transition.

In their initial report of the 3D structure of the Ca^{2+}-ATPase, Toyoshima and co-workers emphasized the central position in the structure of the L6-7 loop, located halfway between the membrane domain and the P domain. They also noticed that residues of this loop were engaged in an extended network of hydrogen bonds, suggesting that the L6-7 loop might play an important role during the Ca^{2+}-dependent phosphorylation from ATP, by transmitting to the P domain the movements of M6 or M5 induced by calcium binding (14). Zhang and colleagues subsequently reported that this hydrogen bond network was indeed critical to stabilize the phosphorylation and calcium binding domains (23).

A well documented example of a functional interplay between the nucleotide binding and Ca^{2+} binding domains is the acceleration by bound nucleotide of the rate of the $E2 \rightarrow E1Ca_2$ conversion (65,67,68,70,80,81). Nucleotide binding to the cytosolic portion of Ca^{2+}-ATPase in the absence of Ca^{2+} apparently permits faster reorganization of the transmembrane domain, leading to faster binding of calcium and/or release of previously occluded protons. The fact, shown here, that the D813A-D818A mutation appreciably reduces the affinity of the ATPase for binding of ATP as well as Ca^{2+}, and simultaneously slows down the $E2 \rightarrow E1Ca_2$ transition step (a slowing down which is reversed at high ATP concentration), could therefore be an indication that the mutation prevents movements of the TM segments with consequences in the distant nucleotide binding domain. As the L6-7 loop seems to essentially follow the P-domain reorientation during the $E2 \rightarrow E1Ca_2$ transition, it is indeed quite conceivable that alterations in this loop, e.g. those induced by the ADA mutation, have consequences on that reorientation, although transmission of information between the nucleotide binding site and the TM domain remains possible with the mutated loop (as shown by the fact that the $E2 \rightarrow E1Ca_2$ transition is accelerated in the presence of high ATP for the mutant, too). The L6-7 loop may thus have a direct contribution in relaying distant conformational changes from one site to the other. This, of course, does not exclude the participation of neighbouring elements, such as the upper part of the M5 transmembrane span, as major conformational changes of the ATPase obviously require concerted changes of the various domains of the protein. Further progress remains to be done to get a better understanding of such a mechanism at the atomic level.

Abbreviations

SR, sarcoplasmic reticulum; SERCA1a, 1a isoform of the SR Ca^{2+}-ATPase; WT, wild type SERCA1a Ca^{2+}-ATPase; ADA, Asp813Ala-Asp818Ala double mutant of SERCA1a; NTA, Ni^{2+}-nitrilotriacetic acid; DDM, β-D-dodecyl maltoside; EYPC, egg yolk L-α-phosphatidylcholine; EYPA, egg yolk phosphatidic acid; EDTA, ethylenediamine tetraacetic acid; EGTA, ethylene glycol-bis(2-aminoethyl)-N,N,N',N'-tetraacetic acid; FITC, fluorescein isothiocyanate; TCA, trichloracetic acid; PAGE, polyacrylamide gel electrophoresis; TEMED, N,N,N',N'-Tetramethylethylenediamine; RPM, revolutions per minute; SDS, sodium dodecyl sulphate; TM, transmembrane; $C_{12}E_8$, octaethylene glycol monododecyl ether; Tes, 2- {[2-hydroxy-1,1-bis(hydroxymethyl)ethyl]amino}ethanesulfonic acid; Hepes, 4-(2-Hydroxyethyl)piperazine-1-ethanesulfonic acid; Mops, 4-Morpholinepropanesulfonic acid; Tg, thapsigargin; cmc, critical micellar concentration; TCA, trichloracetic acid.

Acknowledgements

We would like to thank Cedric Montigny for technical help, Dr. Jean-Marc Verbavatz (LTMD, CEA Saclay, France) for the freeze fracture electron microscopy, Dr. M. Garrigos (LTMD, CEA Saclay, France) for introducing us to the Pi colorimetric measurements in multi-well microtiter plates, Pr. J. P. Andersen (Aarhus University, Denmark) for the gift of SimZyme software, Dr. J-M Neumann (LBPM, CEA Saclay, France) for comments about the structure of the L6-7 region, and Dr. B de Foresta (LTMD, CEA Saclay, France) and Dr. J-J Lacapère (Inserm U410 Unit) for critical discussions and reading of the manuscript. This work was supported by the Commissariat à l'Energie Atomique (CEA), by the "Centre National de la Recherche Scientifique", by Human Frontier Science Program Organization funds (to M. P.) and by a fellowship of the "Ministère de la Recherche et de la Technologie" and from the "*Fondation pour la Recherche Médicale*" (to G. L.).

References

R

1. Hasselbach, W., and Makinose, M. (1961) *Biochemische Zeitschrift* **333**, 518-528
2. Ebashi, S., and Lipman, F. (1962) *The Journal of Cell Biology* **14**, 389-400
3. MacLennan, D. H. (1970) *J. Biol. Chem.* **245**, 4508-4518
4. Mintz, E., and Guillain, F. (1997) *Biochim. Biophys. Acta* **1318**, 52-70
5. MacLennan, D. H., Rice, W. J., and Green, N. M. (1997) *J. Biol. Chem.* **272**, 28815-28818
6. Møller, J. V., Juul, B., and le Maire, M. (1996) *Biochim. Biophys. Acta* **1286**, 1-51
7. Makinose, M. (1973) *FEBS Lett.* **37**, 140-143
8. de Meis, L., and Vianna, A. L. (1979) *Annu. Rev. Biochem.* **48**, 275-292
9. Champeil, P. (1996) in *Biomembranes, ATPases* (Lee, A. G., ed) Vol. 5, pp. 43-76, JAI Press, London
10. Scarborough, G. A. (2002) *J. Bioenerg. Biomembr.* **34**, 235-250
11. MacLennan, D. H., Brandl, C. J., Korczak, B., and Green, N. M. (1985) *Nature* **316**, 696-700
12. Zhang, P., Toyoshima, C., Yonekura, K., Green, N. M., and Stokes, D. L. (1998) *Nature* **392**, 835-839
13. Dux, L., Pikula, S., Mullner, N., and Martonosi, A. (1987) *J. Biol. Chem.* **262**, 6439-6442
14. Toyoshima, C., Nakasako, M., Nomura, H., and Ogawa, H. (2000) *Nature* **405**, 647-655
15. Toyoshima, C., and Nomura, H. (2002) *Nature* **418**, 605-611
16. Martonosi, A. N., and Pikula, S. (2003) *Acta Biochim. Pol.* **50**, 337-365
17. Clarke, D. M., Loo, T. W., Inesi, G., and MacLennan, D. H. (1989) *Nature* **339**, 476-478
18. Andersen, J. P. (1995) *Biosci. Rep.* **15**, 243-261
19. Falson, P., Menguy, T., Corre, F., Bouneau, L., de Gracia, A. G., Soulié, S., Centeno, F., Møller, J. V., Champeil, P., and le Maire, M. (1997) *J. Biol. Chem.* **272**, 17258-17262
20. Menguy, T., Corre, F., Bouneau, L., Deschamps, S., Møller, J. V., Champeil, P., le Maire, M., and Falson, P. (1998) *J. Biol. Chem.* **273**, 20134-20143
21. Menguy, T., Corre, F., Juul, B., Bouneau, L., Lafitte, D., Derrick, P. J., Sharma, P. S., Falson, P., Levine, B. A., Møller, J. V., and le Maire, M. (2002) *J. Biol. Chem.* **277**, 13016-13028
22. Zhang, Z., Lewis, D., Strock, C., Inesi, G., Nakasako, M., Nomura, H., and Toyoshima, C. (2000) *Biochemistry* **39**, 8758-8767
23. Zhang, Z., Lewis, D., Sumbilla, C., Inesi, G., and Toyoshima, C. (2001) *J. Biol. Chem.* **276**, 15232-15239

24. Xu, G., Farley, R. A., Kane, D. J., and Faller, L. D. (2003) *Ann. N. Y. Acad. Sci.* **986**, 96-100
25. Costa, V., and Carloni, P. (2003) *Proteins* **50**, 104-113
26. Andersen, J. P., Clausen, J. D., Einholm, A. P., and Vilsen, B. (2003) *Ann. N. Y. Acad. Sci.* **986**, 72-81
27. Falson, P., Lenoir, G., Menguy, T., Corre, F., Montigny, C., Pedersen, P. A., Thinès, D., and Le Maire, M. (2003) *Ann. N. Y. Acad. Sci.* **986**, 312-314
28. Lenoir, G., Menguy, T., Corre, F., Montigny, C., Pedersen, P. A., Thinès, D., le Maire, M., and Falson, P. (2002) *Biochim. Biophys. Acta* **1560**, 67-83
29. Lenoir, G., Montigny, C., Le Maire, M., and Falson, P. (2003) *Ann. N. Y. Acad. Sci.* **986**, 333-334
30. de Meis, L., and Hasselbach, W. (1971) *J. Biol. Chem.* **246**, 4759-4763
31. Champeil, P., Guillain, F., Venien, C., and Gingold, M. P. (1985) *Biochemistry* **24**, 69-81
32. Cuenda, A., Henao, F., Nogues, M., and Gutierrez-Merino, C. (1994) *Biochim. Biophys. Acta* **1194**, 35-43
33. MacDonald, R. C., MacDonald, R. I., Menco, B. P., Takeshita, K., Subbarao, N. K., and Hu, L. R. (1991) *Biochim. Biophys. Acta* **1061**, 297-303
34. Pullman, M. E., Penefsky, H. S., Datta, A., and Racker, E. (1960) *J.Biol. Chem.* **235**, 3322-3329
35. Møller, J. V., Lind, K. E., and Andersen, J. P. (1980) *J. Biol. Chem.* **255**, 1912-1920
36. Lund, S., Orlowski, S., de Foresta, B., Champeil, P., le Maire, M., and Moller, J. V. (1989) *J. Biol. Chem.* **264**, 4907-4915
37. Tsien, R., and Pozzan, T. (1989) *Methods Enzymol.* **172**, 230-262
38. Drueckes, P., Schinzel, R., and Palm, D. (1995) *Anal. Biochem.* **230**, 173-177
39. Saheki, S., Takeda, A., and Shimazu, T. (1985) *Anal. Biochem.* **148**, 277-281
40. Vyskocil, F., Teisinger, J., and Dlouha, H. (1980) *Nature* **286**, 516-517
41. Vijaya, S., and Ramasarma, T. (1985) *J. Inorganic Biochemistry* **20**, 247-254
42. Molnar, E., Kiss, Z., Dux, L., and Guba, F. (1988) *Acta Biochim. Biophys. Hung.* **23**, 63-74
43. Guillain, F., Gingold, M. P., and Champeil, P. (1982) *J. Biol. Chem.* **257**, 7366-7371
44. Sarkadi, B., Enyedi, A., Foldes-Papp, Z., and Gardos, G. (1986) *J. Biol. Chem.* **261**, 9552-9557
45. Weber, K., and Osborn, M. (1969) *J. Biol. Chem.* **244**, 4406-4412
46. Laemmli, U. K. (1970) *Nature* **227**, 680-685
47. Menguy, T., Chenevois, S., Guillain, F., le Maire, M., Falson, P., and Champeil, P. (1998) *Anal. Biochem.* **264**, 141-148

48. Lenoir, G., M., P., C., G., C., M., Le Marechal, P., P., F., M., l. M., V., M. J., and P., C. (2004) *J. Biol. Chem.* **in press**
49. Smith, P. K., Krohn, R. I., Hermanson, G. T., Mallia, A. K., Gartner, F. H., Provenzano, M. D., Fujimoto, E. K., Goeke, N. M., Olson, B. J., and Klenk, D. C. (1985) *Anal Biochem* **150**, 76-85
50. Sørensen, T. L., and Andersen, J. P. (2000) *J. Biol. Chem.* **275**, 28954-28961
51. Andersen, J. P., Sorensen, T. L., Povlsen, K., and Vilsen, B. (2001) *J. Biol. Chem.* **276**, 23312-23321
52. Fujimori, T., and Jencks, W. P. (1992) *J. Biol. Chem.* **267**, 18466-18474
53. Orlowski, S., and Champeil, P. (1993) *FEBS Lett.* **328**, 296-300
54. Andersen, J. P., Le Maire, M., Kragh-Hansen, U., Champeil, P., and Moller, J. V. (1983) *Eur. J. Biochem.* **134**, 205-214
55. de Foresta, B., le Maire, M., Orlowski, S., Champeil, P., Lund, S., Moller, J. V., Michelangeli, F., and Lee, A. G. (1989) *Biochemistry* **28**, 2558-2567
56. de Foresta, B., Henao, F., and Champeil, P. (1994) *Eur. J. Biochem.* **223**, 359-369
57. Dupont, Y., Guillain, F., and Lacapère, J. J. (1988) *Methods Enzymol.* **157**, 206-219
58. Miras, R., Cuillel, M., Catty, P., Guillain, F., and Mintz, E. (2001) *Protein Expr Purif* **22**, 299-306
59. Forge, V., Mintz, E., and Guillain, F. (1993) *J. Biol. Chem.* **268**, 10953-10960
60. Pick, U. (1982) *J Biol Chem* **257**, 6111-6119
61. Lacapère, J. J., Gingold, M. P., Champeil, P., and Guillain, F. (1981) *J. Biol. Chem.* **256**, 2302-2306
62. Andersen, J. P., and Vilsen, B. (1994) *J. Biol. Chem.* **269**, 15931-15936
63. Nakamura, Y. (1984) *J Biol Chem* **259**, 8183-8189
64. Orlowski, S., Lund, S., Møller, J. V., and Champeil, P. (1988) *J. Biol. Chem.* **263**, 17576-17583
65. Carvalho, C. A., and Santos, M. S. (1976) *Experientia* **32**, 428-430
66. de Meis, L. (1976) *J. Biol. Chem.* **251**, 2055-2062
67. Scofano, H. M., Vieyra, A., and de Meis, L. (1979) *J. Biol. Chem.* **254**, 10227-10231
68. Stahl, N., and Jencks, W. P. (1984) *Biochemistry* **23**, 5389-5392
69. Wakabayashi, S., and Shigekawa, M. (1990) *Biochemistry* **29**, 7309-7318
70. Mintz, E., Mata, A. M., Forge, V., Passafiume, M., and Guillain, F. (1995) *J. Biol. Chem.* **270**, 27160-27164
71. Sørensen, T., Vilsen, B., and Andersen, J. P. (1997) *J. Biol. Chem.* **272**, 30244-30253
72. Sørensen, T. L.-M., Dupont, Y., Vilsen, B., and Andersen, J. P. (eds) (2000) *Fast kinetic measurments of mutational effects on conformational changes in SR Ca^{2+}-ATPase.* Na/K

ATPase and Related ATPases. Edited by Kaya, K. T. S. 1207 vols., Excerpta Medica-Elsevier Science, Amsterdam
73. Karlish, S. J., Beauge, L. A., and Glynn, I. M. (1979) *Nature* **282**, 333-335
74. Andersen, J. P., and Møller, J. V. (1985) *Biochim. Biophys. Acta* **815**, 9-15
75. Ortiz, A., Garcia-Carmona, F., Garcia-Canovas, F., and Gomez-Fernandez, J. C. (1984) *Biochem. J.* **221**, 213-222
76. Lacapère, J. J., Bennett, N., Dupont, Y., and Guillain, F. (1990) *J. Biol. Chem.* **265**, 348-353
77. Zhang, X., Cui, Z., Miyakawa, T., and Moye-Rowley, W. S. (2001) *J Biol Chem* **276**, 8812-8819
78. de Foresta, B., Henao, F., and Champeil, P. (1992) *Eur. J. Biochem.* **209**, 1023-1034
79. Cantilina, T., Sagara, Y., Inesi, G., and Jones, L. R. (1993) *J. Biol. Chem.* **268**, 17018-17025
80. Inesi, G., Kurzmack, M., Coan, C., and Lewis, D. E. (1980) *J. Biol. Chem.* **255**, 3025-3031
81. Lacapère, J. J., and Guillain, F. (1993) *Eur. J. Biochem.* **211**, 117-126
82. Wakabayashi, S., Ogurusu, T., and Shigekawa, M. (1990) *Biochemistry* **29**, 10613-10620
83. Forge, V., Mintz, E., and Guillain, F. (1993) *J. Biol. Chem.* **268**, 10961-10968
84. Duchesne, L., Hubert, J. F., Verbavatz, J. M., Thomas, D., and Pietrantonio, P. V. (2003) *Eur. J. Biochem.* **270**, 422-429

Figure legends

Figure 1. Ni-NTA affinity purification of WT and ADA mutated Ca^{2+}-ATPases expressed in yeast.

Purification was performed as described under "Experimental Procedures". After reconstitution into liposomes, about 2 µg of purified ATPase was loaded on an 8 % polyacrylamide gel and separated by SDS-PAGE according to Laemmli (46). Gels were stained with Coomassie blue after migration. *Lane "LMW"*: low molecular weight standard proteins with the indicated molecular weights. *Lane "Mb"*: yeast light membranes expressing about 2 % WT Ca^{2+}-ATPase; *lane "WT"*: Ni-NTA purified WT Ca^{2+}-ATPase; *lane "ADA"*: Ni-NTA purified ADA mutated Ca^{2+}-ATPase. *Lanes "SR"*: SR vesicles, as indicated.

Figure 2. Ca^{2+}-dependent ATPase activity of purified and reconstituted WT or ADA Ca^{2+}-ATPase, in the presence or absence of solubilizing concentration of $C_{12}E_8$ (or DDM).

A, the rates of ATP hydrolysis by purified and reconstituted WT (circles) or ADA (squares) Ca^{2+}-ATPase were measured as described in "Experimental Procedures" in the presence of a solubilizing concentration (2 mM) of $C_{12}E_8$ or DDM (*inset*). *B*, Conditions were as in Panel A, except that Ca^{2+}-dependent (or Sr^{2+}-dependent, for the *inset*) ATPase activity of purified and reconstituted WT or ADA Ca^{2+}-ATPase was measured without adding any detergent to the assay medium. Data were fitted to a Hill equation.

Figure 3. Effect of $C_{12}E_8$ and β-dodecyl maltoside on WT and ADA Ca^{2+}-ATPase activities.

The rate of ATP hydrolysis by purified and reconstituted WT (circles) or ADA (squares) ATPase was measured in the presence of 0.1 mM Ca^{2+}, 1 mM ATP, and increasing concentrations of either $C_{12}E_8$ (panel A) or DDM (panel B). Detergent cmc has been indicated with arrows.

Figure 4. Ca^{2+}- or Sr^{2+}-dependence of ATPase intrinsic fluorescence changes, and affinity for Ca^{2+} at equilibrium.

A, B, tryptophan fluorescence changes upon calcium (A) or strontium (B) binding to WT or ADA mutated ATPase. Purified and reconstituted WT and ADA Ca^{2+}-ATPases were diluted 20 times into 150 mM Mops-Tris pH 7.0 at 20 °C. Total Ca^{2+} was 55 µM, due to contaminating Ca^{2+} and Ca^{2+} added together with the enzyme. A concentration of 500 µM EGTA was added first to reduce the free Ca^{2+} concentration to 0.05 µM and then successive additions of 300 µM $CaCl_2$ allowed to reach 1, 155 and 455 µM of $[Ca^{2+}]_{free}$, as calculated using a $Kd_{Ca\text{-}EGTA}$ of 0.4 µM. The fluorescence levels of WT and ADA ATPases have been expressed as % of their initial value, and slightly shifted with respect to each other for clarity. The very small changes (typically 0.1-0.2 %) due to dilution were corrected for. Additions were identical for WT and ADA ATPases, as indicated by the dotted lines. *C, Ca^{2+}-dependence of the normalized fluorescence changes*. Fluorescence changes of WT (circles) and ADA (squares) were plotted, considering as 100 % the difference between the initial fluorescence level in the presence of 55 µM Ca^{2+} and that in the presence of excess EGTA (closed diamond). Results obtained with SR Ca^{2+}-ATPase (triangles) are also plotted. Data were fitted to a Hill equation.

Figure 5. Ca^{2+}- or vanadate-dependent conformational changes in WT and ADA ATPases, observed after FITC-labelling.

WT and ADA enzymes were labelled with FITC as described under "Experimental Procedures". *A*, *FITC fluorescence changes upon calcium binding to WT and ADA mutated*

ATPases (or its dissociation). After labelling and elimination of unbound FITC with a PD-10 column, WT and ADA ATPases were diluted 5 times into 150 mM Mops-Tris, 100 mM KCl and 5 mM Mg^{2+} (pH 7.0 at 20 °C). Total Ca^{2+} was then 25 µM, taking into account 5 µM contaminating Ca^{2+} and 20 µM Ca^{2+} added with the enzyme. A concentration of 500 µM EGTA was added first to reduce the free Ca^{2+} concentration to 0.02 µM, which was then increased to 0.9 and 125 µM by two successive additions of 300 µM $CaCl_2$ and finally to 1.125 mM by adding 1 mM $CaCl_2$, using an apparent $K_{dCa\text{-}EGTA}$ of 0.5 µM in the presence of 5 mM $MgCl_2$. Additions were identical for WT and ADA ATPases as symbolized by the dotted lines. *B, FITC fluorescence changes upon vanadate and Ca^{2+} binding*. Sequential additions were performed as follows: 300 µM EGTA, 100 µM orthovanadate, 375 µM total Ca^{2+} (100 µM free Ca^{2+}) and, in the case of the ADA mutant only, a final addition of 1 mM Ca^{2+}. The curves have been slightly shifted with respect to each other, for clarity.

Figure 6. Tryptophan fluorescence changes upon addition of inorganic phosphate to reconstituted WT and ADA ATPases. Ca^{2+}-dependence of WT and ADA phosphorylation from [^{32}P]Pi.

A, changes in tryptophan fluorescence upon addition of inorganic phosphate were monitored using purified and reconstituted WT and ADA Ca^{2+}-ATPases, diluted 20 times into 150 mM Mops-Tris, pH 7.0 (20 °C), 5 mM Mg^{2+} and 20 % Me_2SO; total Ca^{2+} was 55 µM, due to contaminating Ca^{2+} and Ca^{2+} added together with the enzyme. A concentration of 0.5 mM EGTA was first added in order to generate a Ca^{2+}-deprived ATPase able to react with Pi, and then various amounts of Pi were sequentially added, to reach total Pi concentrations of 50 µM and 200 µM. A concentration of 1 mM Ca^{2+} (550 µM free Ca^{2+}) was finally added to restore the $E1Ca_2$ fluorescence level.

B, C, for phosphorylation experiments from [^{32}P]Pi, the medium contained 20 % Me_2SO, 20 mM $MgCl_2$ and 100 mM Mops-Tris, pH 7.0 (20 °C). The reaction was carried out at the indicated $[Ca^{2+}]_{free}$ and stopped after 30 seconds by acid quenching, as described under « Experimental Procedures ». Samples were run on SDS-PAGE gels using the Sarkadi or Weber-Osborn's method (gels corresponding to the latter method are shown), and phosphorylation was measured and plotted (*Panel C*) for WT (circles) and ADA (squares). Data are average values corresponding to 3 independent experiments and were fitted to a Hill equation.

Figure 7. Limited activation of ADA ATPase at low ATP concentration.

A, B, steady-state Ca^{2+}-dependent phosphorylation from ATP of WT and ADA ATPases. WT (circles) or ADA (squares) was incubated with 2 µM of [γ-^{32}P]ATP at 20 °C at the indicated Ca^{2+}-free concentrations, as detailed under "Experimental Procedures". Samples were acid-quenched after 15 seconds of incubation and radioactivity was quantified after electrophoretic separation, using a PhosphorImager. *C, ATP hydrolysis by WT and ADA ATPases at the same low ATP concentration*. Here, the ATPase activity of WT (circles) and ADA (squares) was measured in the presence of 2 µM Na_2ATP only. For comparison, controls performed in the presence of 1 mM ATP (i.e. as in Figure 2B) in the same series of experiments are shown in the inset.

Figure 8. Rates of phosphorylation and dephosphorylation from [γ-^{32}P]ATP.

A, transient overshoot in phosphorylation at low ATP concentration, as deduced from fast kinetics experiments. WT (circles) or ADA (squares) ATPase was incubated at 2 µg/ml in buffer A supplemented with calcium and EGTA to reach 150 µM free Ca^{2+}. ATPase phosphorylation was then triggered by vol/vol mixing with buffer A supplemented with 4 µM [γ-^{32}P]ATP as well as calcium and EGTA (again to reach 150 µM free Ca^{2+}). The reaction was carried out at 20 °C and then stopped at indicated times by acid-quenching, using a rapid mixing and quenching equipment. Proteins were then separated by electrophoresis as detailed under "Experimental Procedures" and phosphoenzyme formation was detected by autoradiography. The ^{32}P radioactivity counted for the

various lanes was corrected for slight differences in the amount of protein layered on these lanes (as revealed by Coomassie blue staining after migration, not shown). Solid lines correspond to simulation with Simzyme of a three-species scheme; the rate constants used to simulate the various reactions, E2 → Ca_2E1, Ca_2E1 → ΣEP and ΣEP → E2, are indicated as insets (backward rates were set to zero). *B, kinetics of phosphoenzyme overall decay*. Phosphorylation of WT (circles) or ADA (squares) ATPase was first carried out, on ice, with 2 µg/ml of ADA or WT ATPase incubated in buffer A supplemented with calcium, EGTA (to reach 120 µM free Ca^{2+}) and 2 µM [γ-^{32}P]ATP. After 15 seconds of reaction, 100 µM non-radioactive ATP was added to the solution and the reaction was stopped by acid-quenching after various periods of time. Radioactivity was quantified as in Panel A**,** the amount of phosphoenzyme present at the end of the 15-second phosphorylation period being taken as 100 %. Data are average values corresponding to 3 independent experiments.

Figure 9. Vanadate-sensitivity of ATP hydrolysis by purified and reconstituted WT and ADA ATPases.

A, the rates of ATP hydrolysis by purified and reconstituted WT (circles) or ADA (squares) Ca^{2+}-ATPase (or SR vesicles, triangles and dotted lines) were determined by measuring the amount of Pi liberated within 25-50 minutes (see "Experimental Procedures") in a medium containing 50 mM Mops-Tris, pH 7.0 (20 °C), 100 mM KCl, 5 mM Mg^{2+}, 1 mM MgATP, 1 mM phosphoenolpyruvate, 0.1 mg/ml pyruvate kinase, 100 µM Ca^{2+}, 2 µg/ml calcium ionophore A23187, and various concentrations of orthovanadate. *B*, the true affinity with which ATPase is inhibited by orthovanadate was measured as the activity remaining after extended incubation of the membranes in the absence of Ca^{2+} and the presence of various concentrations of orthovanadate together with glycerol (see Experimental Procedures).

Figure 10. Fluorescence changes upon addition of ATP to SR vesicles or reconstituted WT or ADA ATPases: loss of "true" affinity for ATP binding to Ca^{2+}-free ADA enzyme.

Tryptophan fluorescence changes upon addition of ATP were monitored. For Panel *A* experiment, SR vesicles (at 0.1 mg/ml), and for Panel *B* experiment, reconstituted WT (0.16 mg/ml) or ADA (0.2 mg/ml) ATPase, was diluted 20-fold into 150 mM Mops-Tris, pH 7.0 (20 °C) and 5 mM Mg^{2+}. Total Ca^{2+} concentration was adjusted to 55 µM, taking into account contaminating Ca^{2+} and Ca^{2+} added together with the enzyme. After an initial addition of 2 mM EGTA, various amounts of ATP were sequentially added, to reach final concentrations of 5, 55, 105, 155 and 355 µM. Each addition implied dilution by 0.1 % or 0.2 %, which has been corrected for in the Figure. Since the excitation wavelength for tryptophan fluorescence was here kept at 290 nm, addition of the highest concentration of ATP gives rise to a significant inner filter effect, which can be clearly seen, but however remains very small or even negligible for the smallest concentrations.

Supplemental Figures

Figure A. Freeze fracture electron microscopy of purified WT Ca^{2+}-ATPase reconstituted in an EYPC-EYPA mixture.

Experimental conditions were as described in (84).

Figure B. Ca^{2+}-dependent ATPase activity of the purified ADA mutant ATPase, reconstituted with an EYPC-EYPA mixture or with EYPC alone.

Experimental conditions were as in Figure 1, except that ADA ATPase was reconstituted either with EYPC alone (closed symbols) or with the EYPC:EYPA mixture (open symbols).

Figure C. Utilization of Ca^{2+}-ATP as a substrate, instead of MgATP, by ADA or WT at high Ca^{2+} concentrations, as revealed by the kinetics of phosphoenzyme decay. Phosphorylation of SR (triangles), WT (circles) or ADA (squares) ATPase was first carried out, on ice, with 2 µg/ml of ATPase incubated in buffer A supplemented with either 10 mM ("high", closed symbols) or 100 µM ("low", open symbols) free calcium, and 2 µM [γ-^{32}P]ATP. After 15 seconds of reaction, 100 µM non-radioactive ATP was added to the solution and the reaction was stopped by acid-quenching after various periods of time. Radioactivity was quantified with a PhosphorImager as for Panel A in Figure 8**,** the amount of phosphoenzyme present at the end of the 15-second phosphorylation period being taken as 100 %.

Figure D. Vanadate-dependent oxidation of NADH in the absence of any membranes.

NADH oxidation was followed by continuously monitoring its absorbance at 340 nm, in a medium containing 50 mM Mops-Tris at pH 7.0 (20 °C), 100 mM KCl, 5 mM Mg^{2+}, 100 µM Ca^{2+} and 0.3 mM NADH. For the left trace, it also contained 1 mM phosphoenolpyruvate, 0.1 mg/ml pyruvate kinase, 0.1 mg/ml lactate dehydrogenase and 1 mM MgATP. ADP (20 µM) was first added, followed by SR vesicles (2 µg/ml) and A23187 (1 µg/ml). Then, increasing amounts of orthovanadate were added, leading to total concentrations of 30 µM, 330 µM and 1030 µM. Vanadate increased the rate of NADH oxidation instead of demonstrating the expected inhibition of ATPase activity. Right trace, same experiment in buffer alone (without PEP, PK, LDH, ATP or SR membranes), to which vanadate alone was added at the same final concentrations, inducing marked increases in the rate of non enzymatic NADH oxidation (40).

Figure E. Slow reactivation, upon dilution into a vanadate-free assay medium, of ATPase activity previously inhibited by orthovanadate.

SR vesicles were incubated here at 1 mg/ml (plus 20 µg/ml A23187) and at a very low $Ca^{2+}{}_{free}$ concentration (0.1 mM Ca^{2+} + 0.6 mM EGTA) in the absence (left trace) or presence (right trace) of 150 µM orthovanadate, for 10 minutes, and then diluted 100-fold into a standard Ca^{2+}-containing medium for coupled-enzyme assay of the residual ATPase activity (the assay medium contained 50mM Mops-Tris, pH 7.0 (20 °C), 100 mM KCl, 5 mM Mg^{2+}, 1 mM MgATP, 1 mM phosphoenolpyruvate, 0.1 mg/ml pyruvate kinase, 0.1 mg/ml lactate dehydrogenase, 0.3 mM NADH and 100 µM free Ca^{2+}). The addition of 1.5 µM vanadate (arrow) to the left trace did not significantly affect activity.

Fig 1. Ni-NTA affinity purification of WT and ADA mutated Ca^{2+}-ATPases expressed in yeast.

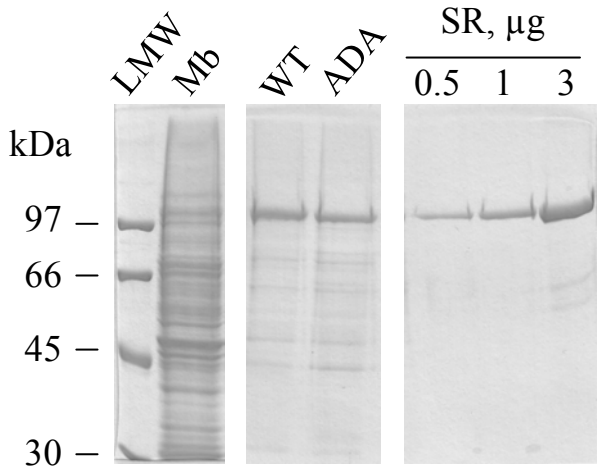

Fig 2. Ca^{2+}-dependent ATPase activity of purified and reconstituted WT and ADA Ca^{2+}-ATPases, in the presence or absence of solubilizing concentrations of $C_{12}E_8$ (or DDM).

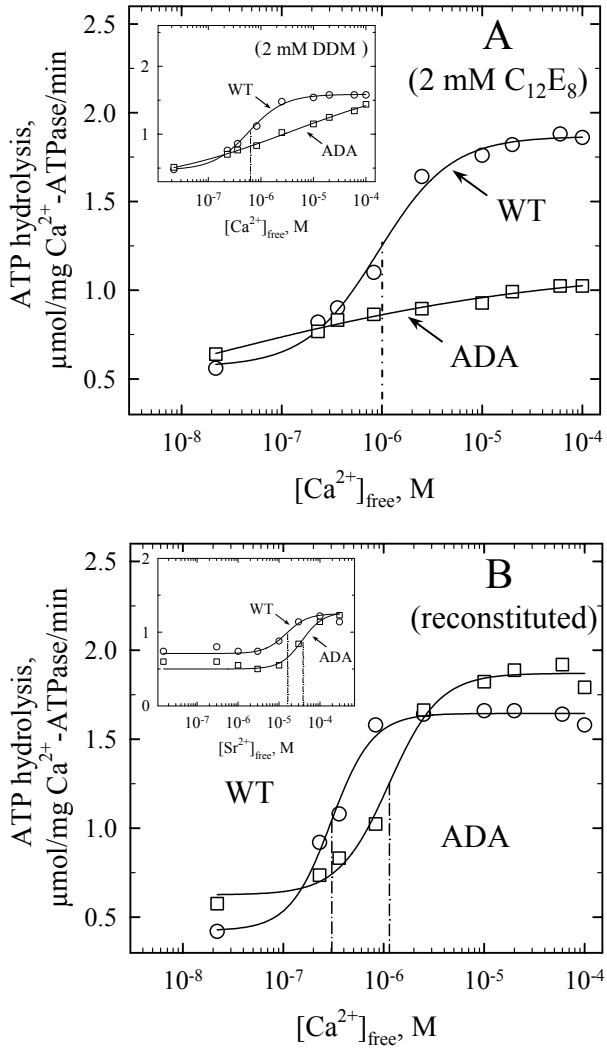

Fig 3. Effect of $C_{12}E_8$ and β-dodecyl maltoside on WT and ADA Ca^{2+}-ATPase activities.

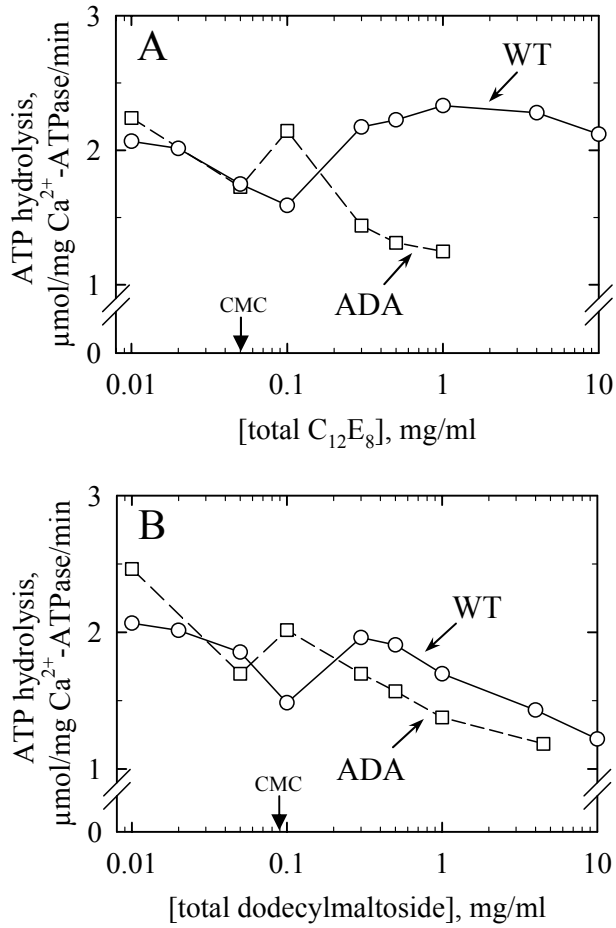

Fig 4. Ca^{2+} or Sr^{2+} dependence of ATPase intrinsic fluorescence changes and measurement of the affinity for Ca^{2+} at equilibrium.

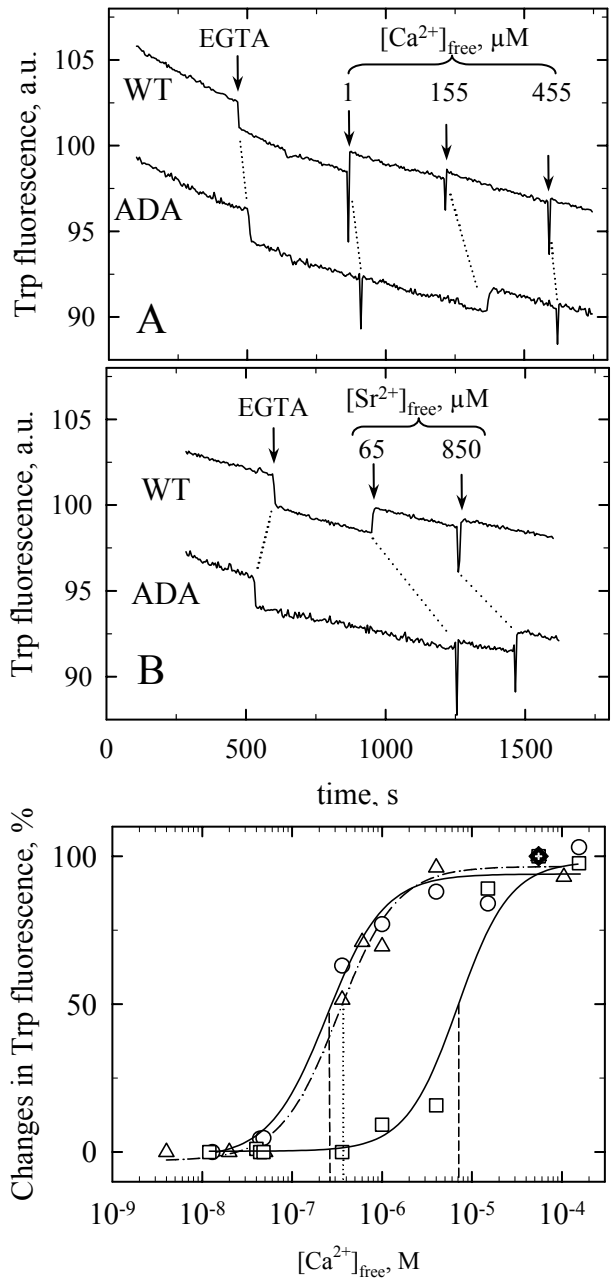

Fig 5. Ca^{2+} and VO_4-dependent conformational changes in FITC-labelled WT and ADA ATPases.

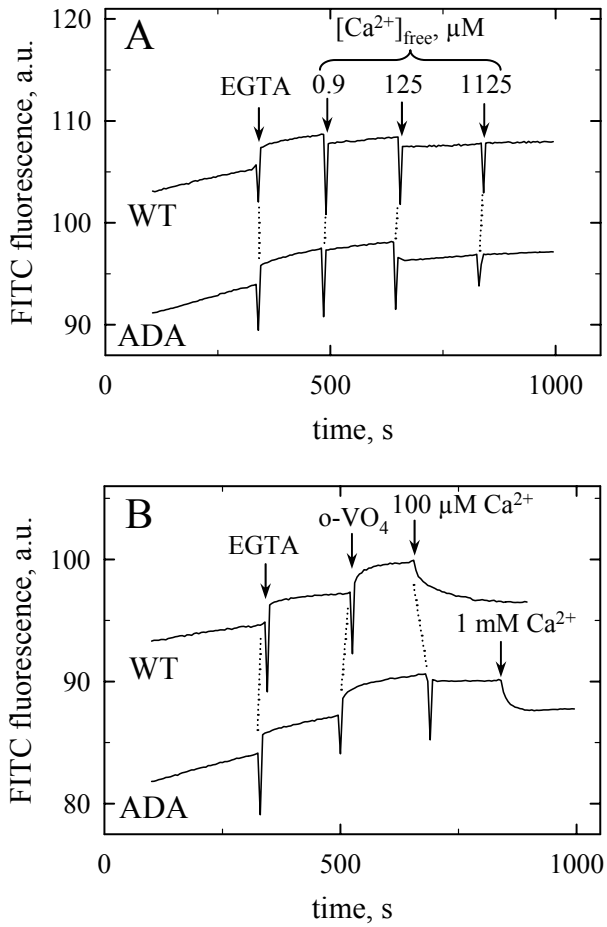

Fig 6. Trp fluorescence changes of WT and ADA ATPases upon addition of inorganic phosphate, and Ca^{2+}-dependence of phosphorylation from [^{32}P]Pi.

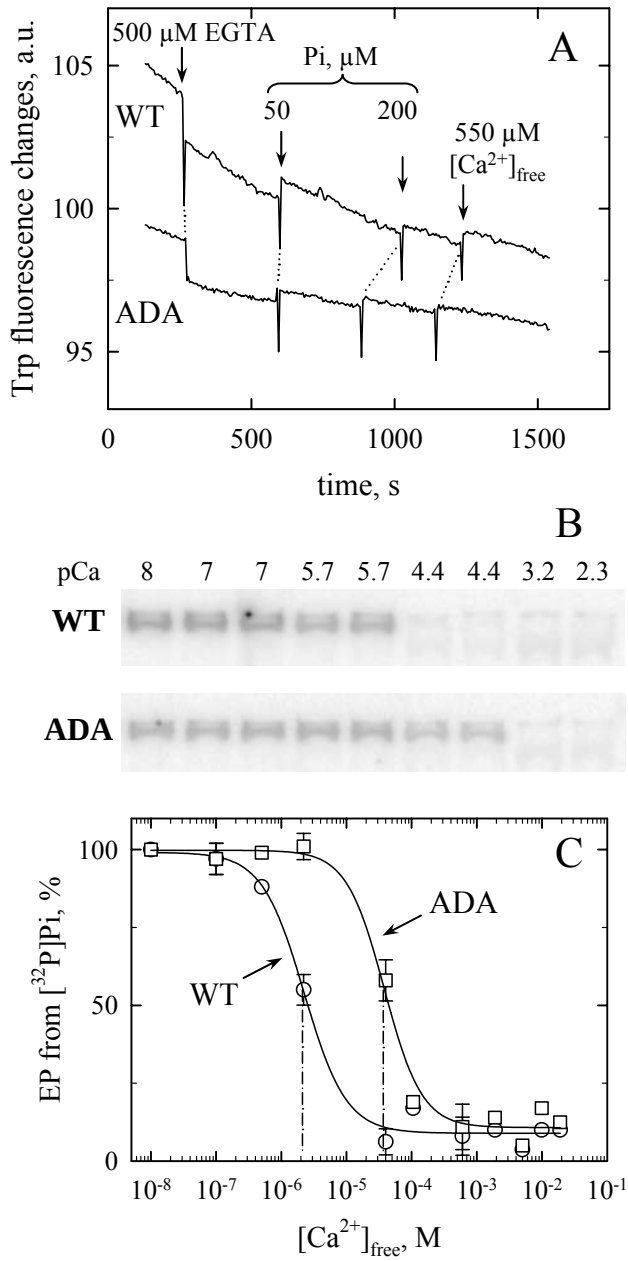

Fig 7. Limited activation of ADA ATPase at low ATP concentration.

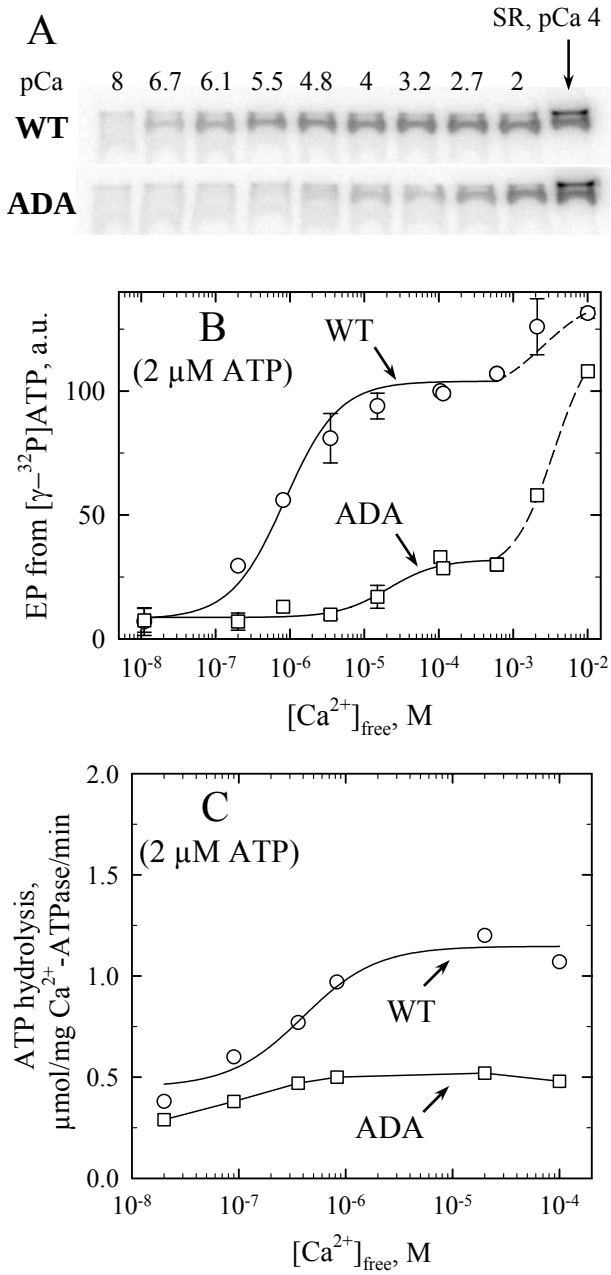

Fig 8. Rates of dephosphorylation and phosphorylation from [γ-^{32}P]ATP

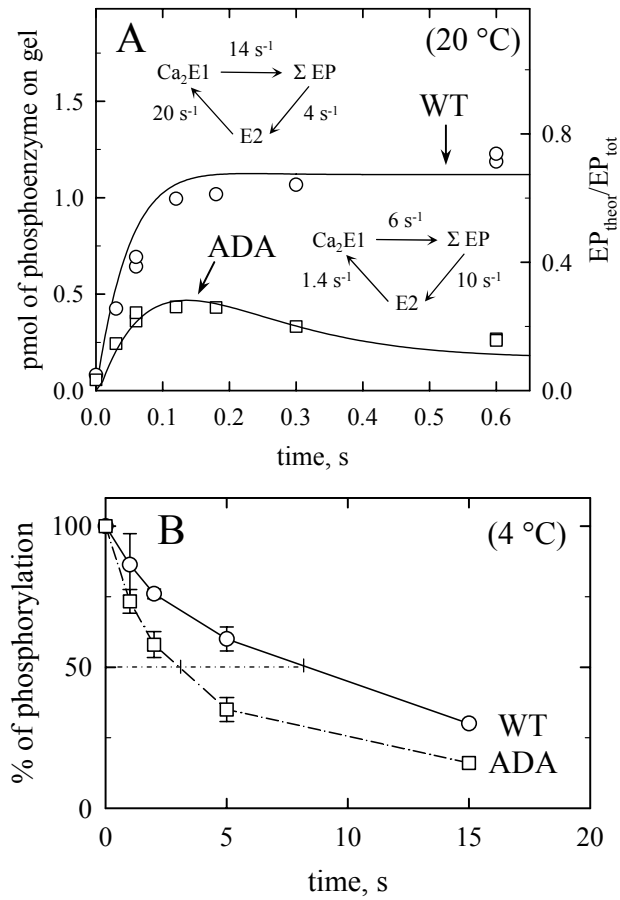

Fig 9. Vanadate-sensitivity of ATP hydrolysis by WT or ADA ATPase.

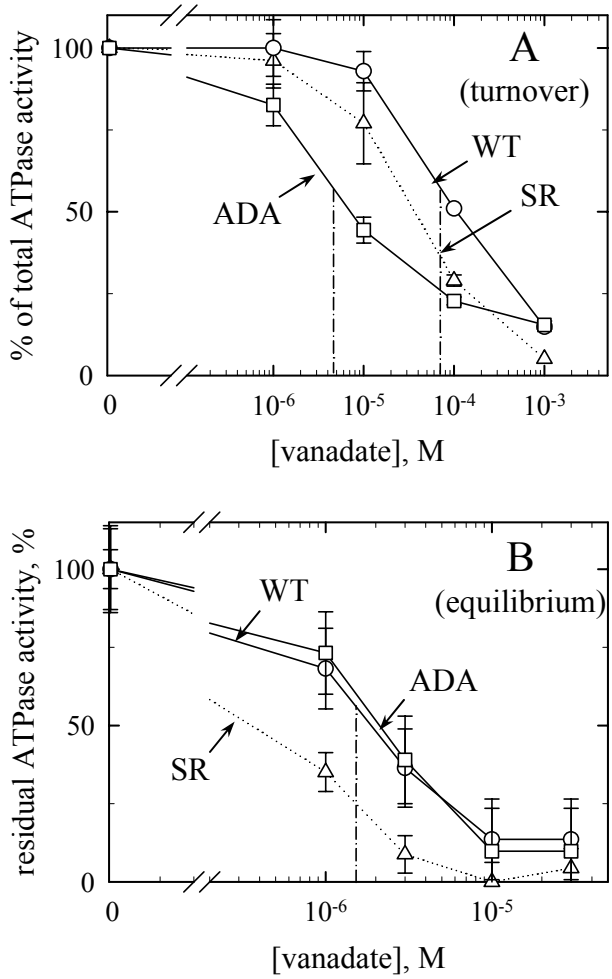

Fig 10. Fluorescence changes upon addition of ATP to SR vesicles and reconstituted WT and ADA ATPases.

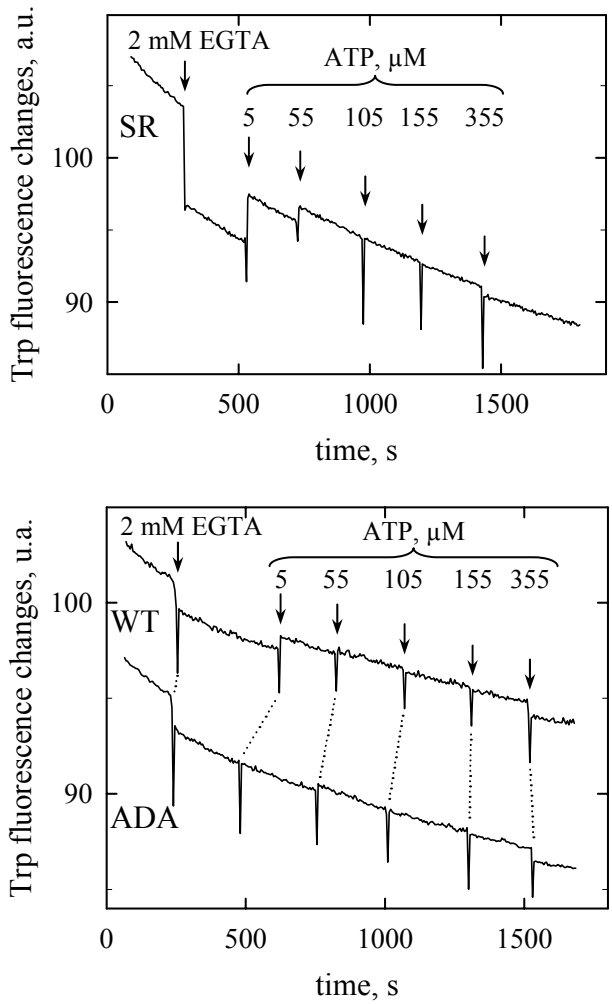

Supplemental material.

Fig A. Freeze fracture electron microscopy

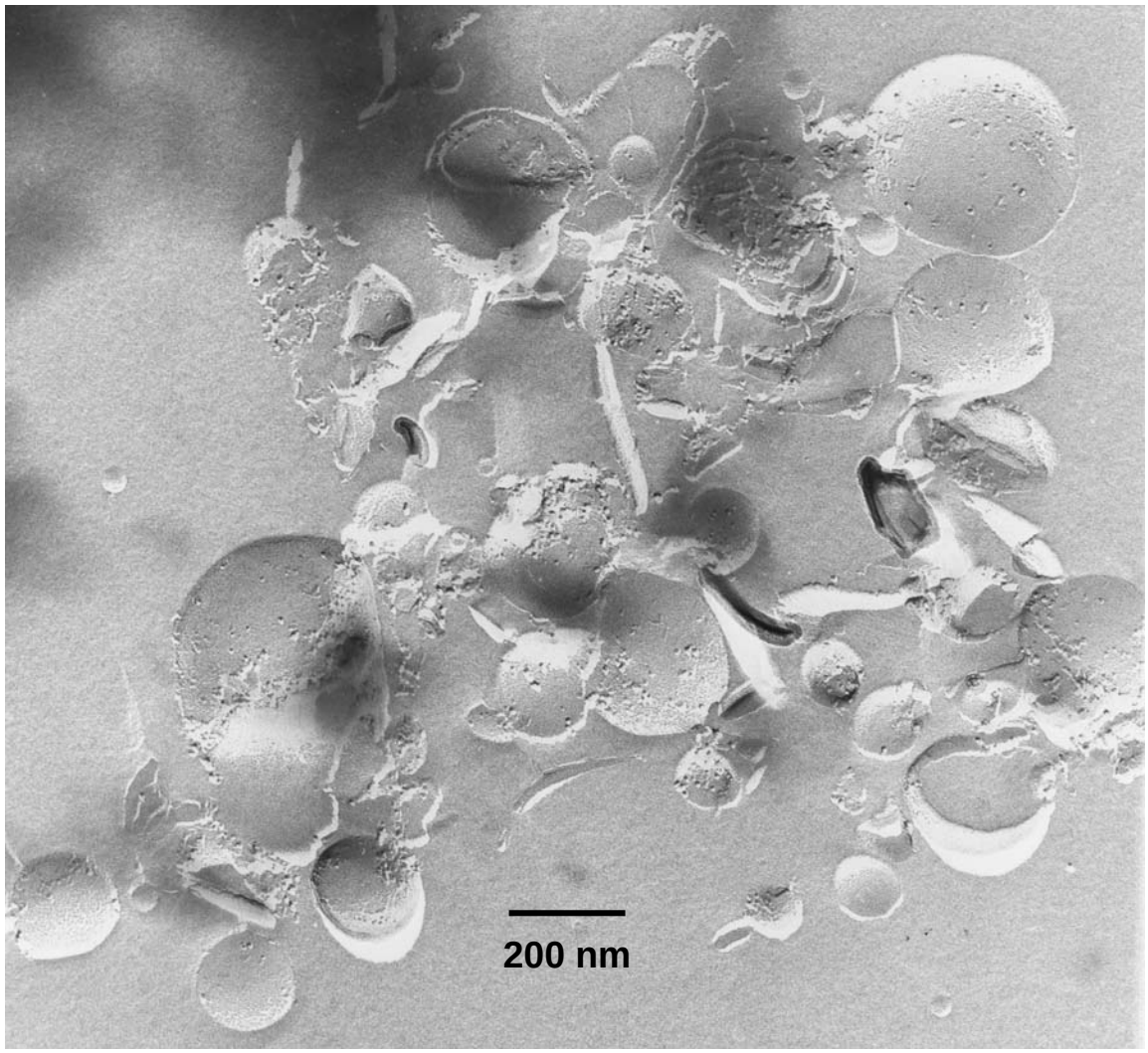

Supplemental material.

Fig B. Ca^{2+}-dependent ATPase activity of purified ADA Ca^{2+}-ATPase reconstituted with EYPC and EYPA or EYPC alone.

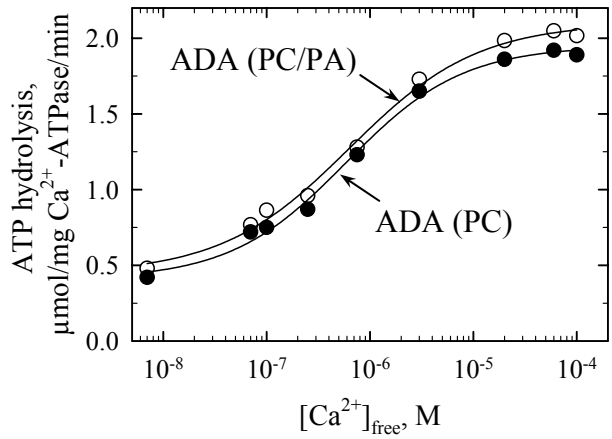

Fig C. Utilization of Ca^{2+}-ATP as a substrate at high Ca^{2+} concentrations.

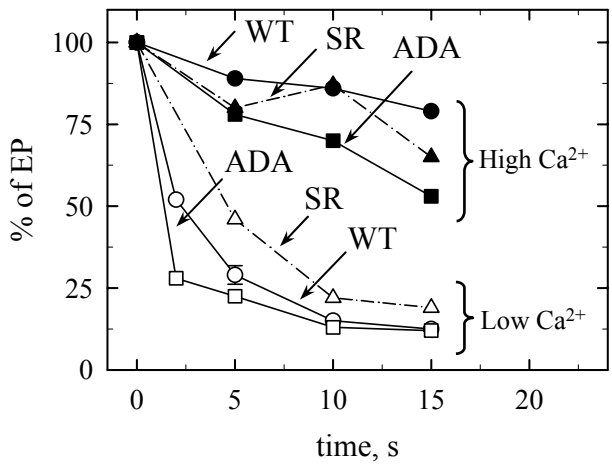

Supplemental material.

Fig D. Vanadate-dependent oxidation of NADH in the presence or absence of membranes.

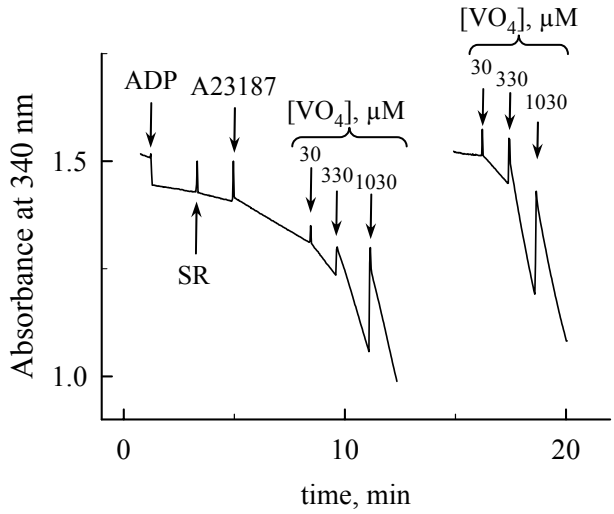

Fig E. Slow reactivation, upon dilution into a vanadate-free assay medium, of ATPase activity previously inhibited by orthovanadate.